Titre: Title:	Dry powder mass flow control of a vibratory micro-L-Valve
Auteur: Author:	Jun Zhu
Date:	2003
Type:	Mémoire ou thèse / Dissertation or Thesis
Référence: Citation:	Zhu, J. (2003). Dry powder mass flow control of a vibratory micro-L-Valve [Mémoire de maîtrise, École Polytechnique de Montréal]. PolyPublie. https://publications.polymtl.ca/7523/

UNIVERSITÉ DE MONTRÉAL

DRY POWDER MASS FLOW CONTROL OF A VIBRATORY MICRO-L-VALVE

JUN ZHU

DÉPARTEMENT DE GÉNIE MÉCANIQUE

ÉCOLE POLYTECHNIQUE DE MONTRÉAL

MÉMOIRE PRÉSENTÉ EN VUE DE L'OBTENTION

DU DIPLÔME DE MAÎTRISE ÈS SCIENCES APPLIQUÉES

(GÉNIE MECANIQUE)

MAI 2003

Library and Archives Canada

Published Heritage Branch

395 Wellington Street
Ottawa ON K1A 0N4
Canada

Bibliothèque et Archives Canada

Direction du Patrimoine de l'édition

395, rue Wellington
Ottawa ON K1A 0N4
Canada

Your file Votre référence
ISBN: 0-612-97993-8
Our file Notre référence
ISBN: 0-612-97993-8

UNIVERSITÉ DE MONTRÉAL

ÉCOLE POLYTECHNIQUE DE MONTRÉAL

Ce mémoire intitulé:

DRY POWDER MASS FLOW CONTROL

OF A VIBRATORY MICRO-L-VALVE

présenté par: ZHU Jun

en vue de l'obtention du diplôme de : Maîtrise ès sciences appliquées

a été dûment accepté par le jury d'examen constitué de:

M. FORTIN Clément, Ph.D., président

M. PEGNA Joseph, Ph.D., membre et directeur de recherche

M. MUREITHI Njuki W., Ph.D, membre

This thesis is dedicated to my beloved parents Anle Zhu and Baozhu Sima. Without their permanent love, support and believing in me this work would have not been possible.

ACKNOWLEDGMENT

I would like to express my sincere appreciation and gratitude to my advisor Dr. Joseph Pegna. It was only under his constant patient guidance and support, that I could successfully overcome many difficulties, which included not only the adaptation to a new language environment, but also the research breakthrough in a completely new scientific field. I still clearly remember the hard time when I newly transferred here from a English speaking university in the autumn, 2000. I could not even find my way out because I did not know that "sortie" meant "exit". It was the constant encouragement from Dr. Joseph Pegna that carried me throughout my study. Moreover, his hardworking trait, precise attitude of work, optimism, sense of humor and his readiness to help other people had a great influence on me and will be my constant inspiration in future endeavors.

I am also grateful to Dr. Aleksandra Drizo, for being ready to help me whenever I needed it. In particular, I would like to thank Aleksandra for her great help with writing up my scientific papers. She was extremely patient in teaching me about structuring of scientific papers, supporting me in my ups and downs, not just as a mentor, but also with her great personality and sense of humor.

I would also like to thank Mr. Francois Ménard and Mr. Sylvain Simard, for their help in fabricating the micro L-Valves throughout the experiments and setting up the powder deposition flowrate measuring system by using LabView. Without their help, the results

would have been delayed for months. I would like to thank Dominique Croteau and Ramkiran Goduguchinta for their help in translating my executive summary into French and carefully correcting my English.

Finally, I would like to thank my friends in Montreal, in particular Jacques Boudreault, Stephen G. Taylor, Yamu Hu, Yang Wang, Shuhua Qin and Muqiao Lv. Being with them has made my life in Montreal for the past three years full of fun.

Above all, many thanks to my wife Lili Liu for being always by my side, for her help, support, understanding, patience and her love.

RÉSUMÉ

Cet ouvrage introduit les premières avancées dans la théorie sous-jacente à un nouvel appareil inventé au sein des Laboratoires de fabrication en forme libre (LFFL) et que nous désignerons par micro L-Valve vibratoire (MLVV). La recherche présentée ici fut initialement formulée dans le contexte des procédés de fabrication en forme libre (FFL) à base de poudres. Toutefois, son impact anticipé dépasse le cadre initial, s'étendant à d'autres applications dans le domaine du contrôle de l'écoulement des matériaux granulaires, dans l'industrie pharmaceutique ou le traitement des poudres métallurgiques.

Dans les procédés commerciaux de FFL par agrégation sélective de poudre tels que le frittage sélectif au laser (FSL) ou l'imprimante 3-D (3DP), des pièces monolithiques sont générées à partir de couches minces de poudre compactées par un rouleau compresseur contre rotatif. Les procédés de FFL par consolidation laser quant à eux, construisent une pièce par projection pneumatique de poudres dans une minuscule flaque de substrat maintenue fondue par laser. Dans les deux cas, le transport et la dépôt de poudres définissent les limites des procédés. Un contrôle précis du débit des poudres est difficile à obtenir et cela affecte les propriétés du produit. La projection des poudres par gaz est notoirement inefficace. Une grande partie de la poudre est inutilisée. De surcroît, les grains de poudres capturés à la périphérie de la focale du laser ne sont que partiellement fondus et reste collés aux parois, affectant le fini de surface. Il est indiscutable que l'aptitude à contrôler les

débits de poudres et leurs dépôts représenterait une avancée majeure en FFL. Cela est l'objectif ultime du programme de recherche auquel cet ouvrage contribue.

La compréhension des mécanismes permettant le contrôle du débit de poudre dans les MLVV constitue l'essentiel de nos travaux de recherche. En bref, une MLVV est constituée d'un micro canal horizontal vibré verticalement. À une extrémité, ce canal est connecté à un réservoir de poudre, à l'autre à une buse de dépôt. Le concept MLVV a été démontré capable de contrôler de façon consistante des débits de poudre de l'ordre de 0.1 à $10 mm^3/s$ par mm^2 de section de canal en modulant la fréquence d'excitation. Toutefois, la MLVV a jusqu'ici été développée de façon purement expérimentale. Jusqu'à nos travaux, il n'y avait aucun modèle théorique expliquant pourquoi et comment la MLVV fonctionne. Ce modèle devrait nous permettre en retour de mieux concevoir les valves en question.

Que ce soit dans les articles de journaux ou les brevets, il n'y a aucune référence sur le contrôle des débits de poudres sèches à faible volume, ni au comportement vibratoire de poudres dans un micro canal. La seule bibliographie qui soit à peu près opportune concerne la réponse vibratoire des lits de poudres, lesquels sont presque toujours modélisés comme une simple particule rebondissant sur une plaque vibrante. La validité d'un tel modèle n'est d'ailleurs testée que dans un seul article expérimental.

Le plan de recherche développé afin d'élucider les mécanismes gouvernant le débit de poudre dans une MLVV consiste premièrement à revisiter le problème d'une particule rebondissant sur une plaque vibrante (ci-après désigné "le problème de simple plaque.") . Cette représentation devra alors être validée par comparaison aux expériences de débit de poudre. En particulier, l'approximation du lit de poudre par une seule particule ne saurait être validée que si la densité de poudre dans le canal est très faible (équivalent à une ou deux épaisseurs de particules environ).

L'obstacle principal à la simulation du problème de simple plaque est d'ordre numérique. En effet, il s'agit de trouver la plus petite racine d'une fonction combinant des polynômes et des fonctions transcendantales. Ce problème est connu pour ne pas avoir de solution analytique et résister aux méthodes numériques. Dans les travaux antérieurs, c'était une source d'incertitude identifiée par certains chercheurs. Une simulation robuste a pu être obtenue toutefois par une nouvelle approche combinant le calcul symbolique et numérique dans laquelle des techniques d'isolations de racines de polynômes étaient appliquées de façon récursive à un développement local en séries de Taylor.

Les travaux antérieurs portant sur le problème de simple plaque avaient identifié la réponse de la particule comme étant chaotique, à l'exception de quelques réponses périodiques instables consistant d'une série de n rebonds. Ces réponses furent désignées comme "périodiques d'ordre n." La robustesse de notre nouvelle approche calculatoire fut

Cette nouvelle capacité nous a non seulement permis de reproduire les travaux d'autres chercheurs, mais nous a permis de découvrir une nouvelle classe de réponses périodiques que nous avons désignées *"réponse souple périodique d'ordre n"* ou par abréviation *"pério-dique d'ordre* $_sn$*."* Dans un mouvement périodique d'ordre $_sn$, la particule exécute une série de n rebonds avant de revenir sur la plaque avec une vitesse relative nulle. La découverte de ce type de réponse nous a amené à constater que les modèles de choc élastique ne sont pas adaptés à la représentation des impacts à très basse vitesse. Une contribution supplémentaire de nos travaux est donc l'introduction d'un nouveau modèle d'impact dans lequel un minimum d'énergie doit être échangé lors de chaque rebond sur la plaque. Cette modification vraiment mineure des lois de la collision élastique s'est révélée avoir de profondes ramifications sur le problème de simple plaque. Au lieu du comportement chaotique qui avait été observé à date et confirmé par nos simulations, nous avons découvert expérimentalement et confirmé par analyse qu'après une période de rebonds apparemment aléatoires, la particule finit par s'établir en mode de réponse périodique d'ordre $_sn$. De plus, pour une fréquence et amplitude données, un seul état périodique est autorisé.

Les mesures de débit expérimentales conduites avec différentes MLVV par balayage en fréquence à amplitude constante sont en accord qualitatif avec nos simulations. À basse fréquence, aucun débit n'est observé. Lorsque la fréquence augmente, le débit commence et continue de croître linéairement jusqu'à un seuil au-delà duquel le débit retombe rapidement pour se stabiliser à haute fréquence.

ABSTRACT

This work presents the first theoretical breakthrough into a novel dry powder flow control device invented in the Freeform Fabrication Laboratories (FFL), called a vibratory micro-L-Valve (VMLV). The research was formulated in the context of powder-based free form fabrication (FFF) processes. However, its anticipated impact overflows into other fields dealing with low granular material flowrates such as pharmaceutical or metallurgical powder treatment.

In commercial *aggregation FFF processes* such as Selective Laser Sintering (SLS) and 3-D Printing (3DP) single-material parts are generated from thin slices of powder spread by compaction with a counter rotating roller. In *laser consolidation FFF processes,* a part is built incrementally by pneumatic projection of powder grains into a small laser melt pool. Powder transport and deposition remains a key process limitation. Accurate feed metering is difficult and alters the quality of the build material. Projection into the melt pool is notoriously inefficient, while unmelted powder grains cause a rough surface finish. The ability to accurately meter powder flowrate and deposit powder patterns would represent a quantum advance in FFF. This constitutes the ultimate objective of the research program to which the present work shall contribute.

This research focuses on understanding the physics underlying dry powder flow metering with a VMLV in order to enable its design and control. In a nutshell, a VMLV consists of

a vertically vibrated horizontal micro-channel connected at one end to a powder reservoir, and at the other to a vertical delivery nozzle. This experimentally-designed VMLV was shown to be capable of repeatable dry powder flowrate control from about 0.1 to $10mm^3/s$ per mm^2 of nozzle cross-section using frequency modulation. However, the VMLV was obtained by iteration through design of experiments. To this point, there was no quantified understanding of why and how this device actually functions.

Be it in the patent or journal literature, there are no references to dry powder flow control at low volumetric flowrates, or to the behavior of granular material in a horizontal micro-channel vibrated vertically. The only relevant bibliographical findings deal with the response of shallow powder beds to vibrations, often modeled after one particle bouncing off a vertically vibrated plate. Such approximation assumes the dominance of interactions between plate and particle over that among particles. The validity of this assumption is only tested in one experimental article.

The plan of investigation to powder flow consisted of first understanding the behavior of a particle bouncing off a vertically vibrated plate (refered to as *"single plate problem"*).

The major computational challenge in simulating the one plate problem lies in finding the smallest root of a rapidly oscillating transcendental-polynomial function. This problem is known to have no analytical solution and to resist numerical methods. It was a source of problems in some of the prior investigations. A robust simulation was derived from a

novel symbolic computation that relied on an original combination of recursive Taylor expansions and root isolation methods.

Prior works on the single plate problem found the response to be chaotic, except in unstable instances called period-n motions, where the particle exhibits a periodic pattern of n bounces. Our novel approach was tested by reproducing previously published simulations. More importantly, the robustness of our computational approach led to the discovery of a new class of motions, called period-$_s n$. In a period-$_s n$ motion, the particle exhibits a stable pattern of n bounces, then lands on the plate with matching velocity. The discovery of period-$_s n$ motions led to the realization that elastic models were not representive of the physics of low-velocity impacts. A further contribution was thus the introduction of a novel model whereby a minimum quantum of kinetic energy must be exchanged at each impact. This minute alterations of the laws of impact mechanics has far reaching ramifications. Instead of the chaotic behavior observed in prior works and confirmed by digital experiments, we found experimentally and confirmed through analysis that after seemingly random bounces, the particle eventually settles in a complex period-$_s n$ motion. Moreover, for a given frequency and amplitude combination, only one periodic motion can exist on the plate.

The experience gained from the one plate problem applies readily to the two-plates. Digital experiments conducted by scanning frequency revealed different responses. At low

frequency, the problem revers to the one plate problem. As the frequency rises, the particle eventually bounces off the upper plate and settles into a periodic motion in phase with the plates. For the most part, the elastic rebound is sufficient to accurately represent the motion. However, as the frequency is scanned, the steady state response reaches points at which the soft landing model must be activated. In those instances, the particle exhibits a complex sub-harmonic motion.

Flowrate measurement experiments conducted with different micro L-valves by scanning frequencies at constant amplitude showed interesting results. At low frequencies, no powder flow was observed. As the frequency rised so did the flowrate until it peaked and went back down to eventually stabilize at a constant low flowrate at high frequencies.

CONDENSÉ EN FRANÇAIS

1 Introduction

L'utilisation et la manipulation de matériau en poudre existe depuis les débuts de l'humanité et fait encore partie de notre quotidien. À l'origine, le dépôt manuele de poudre était utilisée dans la fabrication d'ouvrages en émail et de peinture de sable. Même s'ils ont peu de liens avec les méthodes de fabrication d'aujourd'hui, ces procédés furent les premiers à démontrer la possibilité d'utiliser le dépôt de poudre pour la fabrication d'un objet couche par couche. C'est ainsi que la peinture de sable fût développée comme un art et ce, depuis plus d'un millénaire. C'est en déposant certaines poudres sèches à l'aide d'une gouttière que les Navajo d'Amérique ainsi que les moines du Tibet développèrent cet art pour des motifs religieux.

Mis à part pour la peinture de sable manuelle, de faibles débits massiques de poudre sèche n'ont jamais été atteints dans les établissements industriels. Ces dernières années, la fabrication en forme libre (FFL) a gagné en popularité avec l'apparition de technologies avancées comme le frittage sélectif au laser (SLS), la stéréolithographie (SLA), *laser engineered net shaping* (LENS), l'impression en 3D ainsi que la consolidation laser. L'avancement dans ces technologies nécessitait un contrôle précis du dépôt de poudre.

La L-valve est d'abord constituée d'un goulot vertical finissant en un coude à angle droit. Un fluide pressurisé pourra souffler la poudre par le coude qui s'écoulera ensuite par l'orifice. La L-valve peut contrôler le dépôt de poudre en activant ou désactivant l'injection du fluide, ce qui rendra la poudre fluidifiée ou compactée. Le taux de dépôt typique d'une L-valve est de l'ordre de L/s. L'un des avantages de cette technologie est sa capacité à s'adapter à une très grande variété de débit et de types des matériaux.

Cependant, les L-valves existantes n'ont pas les qualités nécessaires pour obtenir un contrôle précis du dépôt de poudre et ce, pour deux raisons majeures:

1. Le taux de dépôt des appareils existants est de l'ordre de L/s, ce qui est loin de satisfaire les demandes de la FFL qui requiert des taux de dépôt de l'ordre du mg/s.

2. Il est peu probable que la poudre sera déposée en un point seulement lorsqu'elle sera soufflée de l'orifice par le fluide injecté.

À la lumière de l'automatisation et la mécanisation du procédé de peinture avec sable ainsi que par les L-valves, J.Pegna [1997] a developpé et testé le design micro L-valve verticale et vibrante.

En testant différents types de poudre comme le verre granulé, le carbure de silicium en poudre non calibré, le sable et le ciment en poudre, Pegna et al. [23] démontra plusieurs fonctionnalités distinctes de cette micro L-valve qui sont fondamentales afin de pousser plus loin la compréhension du contrôle du debit et du depôt de poudres.

En premier lieu, il a été démontré que ce type de micro L-valve permet de faible taux de dépôt (de l'ordre du mg/s) ce qui n'avait jamais été atteint auparavant dans les installations industrielles. Par ailleurs, il fut observé que le taux de dépôt d'une micro L-valve donnée varie non seulement avec la fréquence de vibration, mais aussi avec les paramètres géométriques de cette valve. Résoudre ces deux facteurs est donc crucial dans l'avancement des procédés de FFL.

2 Revue des travaux antérieurs

Plusieurs chercheurs ont examiné la réponse des matériaux granuleux aux vibrations dans le domaine des vibrations et de l'acoustique [31]-[34]. Cependant, la plupart d'entre eux utilisèrent des approches analytiques ou des simulations numériques et étudier le transport de faible quantité de poudre ne sembla pas attirer de recherche.

Les approches théoriques majeures appliquées par les examinateurs ont formulé l'hypothèse que les interactions entre la poudre et les surfaces prédominent celles entre les particules parce que l'on est en présence de faibles quantités de poudre. Par con-

séquent, le problème du transport de poudre fut simplifié à l'examen de la réaction d'une seule particule qui rebondit sur une plaque.

Le rebondissement de la poudre à l'intérieur d'une micro L-valve n'a pas été examiné en profondeur. De plus, aucune étude n'est rapportée dans la littérature scientifique étudiant le transport des poudres en le simplifiant au problème d'une particule unique rebondissant entre deux plaques. Ceci rend donc le présent travail unique. Pegna et al. [23] ont cependant publié plusieurs articles discutant le potentiel des applications de la micro L-valve dans la fabrication en forme libre (FFL)

3 Simulations numériques

3.1 Une particule unique rebondissant sur une plaque

À la lumière de ces études antérieures, nous avons premièrement développé le modèle d'une particule rebondissant sur une plaque vibrante. En mécanique appliquée, ce modèle est un problème courant et reconnu pour son comportement chaotique. Une méthode de calcul originale combinant des calculs symboliques et des outils d'isolation de racines dans Mathematica™ ont dû être développés pour satisfaire aux exigences de robustesse requises par ce problème.

Certains chercheurs expérimentaux ont rapporté qu'en variant la fréquence de la plaque et en conservant la même amplitude, il y aura au moins une fréquence critique à laquelle le poudre de subira soudainement une expansion. Ce phénomène s'apparente aux mouvements périodiques identifiés par d'autres chercheurs ayant conduit des simulations. Dans un tel cas, les chercheurs considère une seule particule qui retombe à la même position et rebondit avec la même vitesse de départ [31]-[34]. Par ailleurs, quelques chercheurs déclarèrent même qu'il pourrait exister un mouvement de période-2 où la particule répète ses rebondissements sur la plaque à tous les deux bonds adjacents [31]-[34].

Nous avons découvert une autre forme pour le comportement périodique de la particule: lorsqu'elle retombe sur la plaque avec la même vitesse que celle-ci, la particule restera ensuite en contact avec la plaque. Cependant, cette immobilisation ne durera pas indéfiniment et la particule sera à nouveau propulsée dans les airs lorsque l'accélération de la plaque atteindra la même valeur que la gravité.

Exemple: Nous considérons maintenant le cas d'une amplitude de vibration constante A=0.000774 mètres ($7.74X10^{-4}$m). Les cinq premières fréquences correspondantes qui amèneront la particule à atterrir sur la plaque avec une vitesse égale à celle-ci sont: 17.9147Hz, 38.4367Hz, 50.0000Hz, 59.2808Hz et 67.2737Hz. Il est à noter que lorsque l'accélération de la plaque ne peut dépasser l'accélération gravitationnel g, la particule ne pourra être propulsée de nouveau et le premier mode est dans ce cas le sommet de l'onde sinusoïdale.

Les modèles classiques de rebond nous indiquent qu'à chaque fois que la particule atteint la plaque, elle sera propulsée avec une vitesse de sortie proportionnelle à la vi-tesse d'entrée et que l'énergie cinétique sera dissipée mais n'atteindra jamais une valeur nulle. Ce qui est l'équivalent de dire qu'une balle lancée par terre rebondirait sans jamais s'arrêter. D'après les observations de la vie quotidienne, nous savons tous que cela est faux. Il doit donc y avoir une énergie minimale à laquelle une balle entrant en contact avec le sol ne pourra être propulsée de nouveau et restera sur le sol. Nous définirons ce concept comme étant le «modèle d'impact à basse vitesse».

Interprété comme un «attracteur étrange», le modèle d'impact à basse vitesse a un effet quantifiable sur le problème. Aussi longtemps que la vitesse relative entre la particule et la plaque est inférieure à une valeur critique, la particule sera attrapée au moment de l'impact et ne sera propulsée de nouveau que lorsque la plaque atteindra une accélération vers le bas plus grande que g. La particule rebondira ensuite plusieurs fois sur la plaque avant d'être attrapée de nouveau par celle-ci. À chaque fois que la particule sera propulsée de la plaque, elle aura les mêmes conditions initiales (vitesse de départ et hauteur).

Au début, le modèle d'impact à basse vitesse réagit de façon similaire aux modèles classiques en montrant que la particule subit plusieurs mouvements au hasard. Par contre, aussitôt que la vitesse relative d'impact devient suffisamment petite, la particule reste en contact avec la plaque et sera ensuite emprisonnée dans un mouvement périodique. Pour

une combinaison donnée de fréquence et d'amplitude pour la plaque, ce mouvement périodique est unique.

4 Expériences

Pour tester les simulations numériques utilisées dans la section 3, une série d'expériences fut réalisé en montant séparément plusieurs micros L-valves à un vibreur VTS auxquelles on appliqua une vibration verticale à une fréquence inférieure à 100Hz. Le taux de dépôt de poudre fut mesuré via un câble RS232 en utilisant le logiciel LabView™. L'amplitude des plaques fut maintenue à 0.2mm.

Les résultats de l'expérience révélèrent qu'une augmentation de la fréquence de vibration par un facteur de 3.3 (de 30Hz à 100Hz) résulte en l'apparition de trois modes distincts:

1. À des fréquences inférieures à 40Hz, aucun débit de poudre ne fut observé.

2. Entre 40Hz et 55Hz, le taux de dépôt de poudre varie avec la fréquence et subit une augmentation soudaine aux alentours de 48Hz.

3. À des fréquences supérieures à 60Hz, le taux de dépôt de poudre est constant.

L'utilisation de L-valves différentes généra des résultats similaires si l'on considère la répétitivité de l'expérience et la fiabilité de son contrôle. De plus, nous avons remarqué que la masse restante à l'intérieur de la micro L-valve joue un rôle important: losque la valve est presque vide dans ce ces le taux d'écoulement augmente soudainement. Toutes les expériences démontrèrent un comportement similaire, soit une augmentation soudaine dans le taux d'écoulement.

5 Conclusion

Avec le modèle simplifié d'une particule rebondissant sur une plaque, le lit de poudre en surface sur une seule plaque vibrante a été démontré comme étant périodique, contrairement à un problème chaotique comme le voulaient les croyances pré-établies. Pour une combinaison fréquence/amplitude donnée, il n'y a qu'un mode qui puisse exister pour la particule, ce qui explique pourquoi il y a au moins une fréquence critique pour laquelle il y aura une expansion soudaine du lit de poudre en surface lorsque l'on varie la fréquence.

Pour une valve et une amplitude de vibration données, la fréquence a été démontrée comme étant un facteur dominant pour le taux de dépôt de poudre lorsque les vibrations sont à basses fréquences. Cependant, une augmentation de la fréquence n'assurera pas automatiquement une variation du taux de dépôt. À de hautes fréquences, ce taux devient indépendant de la fréquence et reste donc constant. Ceci prouve donc que l'utilisation

des micros L-valves est un très bon choix pour la FFL à cause de leur très bon contrôle et de leur faible taux de dépôt.

Il serait intéressant de poursuivre les recherches afin d'examiner les questions suivantes:

1. Puisque pour une particule rebondissant sur une plaque à une fréquence et amplitude données, la particule ne peut avoir qu'un seul mode de mouvement, il serait nécessaire de faire de plus amples recherches sur la stabilité de cet état.

2. Nous avons déterminé que la géométrie des valves affecte le taux de déposition de poudre. Afin de pouvoir commercialiser la micro L-valve, il nous faudrait donc étudier plus en profondeur ce paramètre.

TABLE OF CONTENTS

LIST OF FIGURES

LIST OF TABLES

INTRODUCTION

This research was formulated in the context of powder-based free form fabrication (FFF) processes, briefly exposed in Section 0.1. It stems from a recognized opportunity to advance the field of FFF significantly with the ability to deposit controled amounts of dry powders in a pointwise manner.

In response to this need, design of experiments [22] conducted by Pegna et al. [23] led to a novel dry powder flow control concept invented within the Freeform Fabrication Laboratories (FFL) at École Polytechnique, called a vibratory micro-L-Valve (VMLV). This approach to metering and depositing small amounts of powder in a controlled manner reached the proof of concept stages. This marks the beginning of the research exposed herein. Design of experiments having reached its limits, we now have to turn to modeling and analysis in order to further the design and optimize the VMLV. In order to recall the history behing our research, Section 0.2 presents a brief background review.

Section 0.3 summarize our bibliographical search. A state of the art review revealed a technological vaccuum in matters of powder deposition, short of the ancient religious practices of sand paintings and mandalas. Be it in the patent or journal literature, neither are there references to dry powder flow control at low volumetric flowrates, nor to the behavior of granular material in a horizontal micro-channel vibrated vertically. The only remotely relevant bibliographical findings deal with the response of shallow powder beds

to vibrations, often modeled after one particle bouncing off a vertically vibrated plate. This is somewhat similar to the vibrated microchannel problem, to the extent that the microchannel can be modeled as a pair of plates. The single particle approximation however assumes the dominance of interactions between plate and particle over that among particles. The validity of this assumption in the one plate problem is only tested in one experimental article.

The rationale and plan of investigation to uncover the mechanisms governing powder flow is exposed in Section 0.4. It consists of understanding the behavior of a particle bouncing off a vertically vibrated plate (referred to as "single plate problem").

In accordance with the plan of investigation, Section 0.5 presents the organization of the manuscript. Chapters 2 will review the theoretical analysis and modeling of a single particle on a vibrating plate. Chapter 4 presents experimental results from flowrate characterization.

The main contributions of this work are summarized in Section 0.4. Our research added to the state of knowledge on the one plate problem, and compared the results to flow characterization experiments.

0.1 Introduction to powder-based Free Form Fabrication processes

Powder-based free form fabrication processes build parts from increments of bulk material, either by selective aggregation or by consolidation.

In commercial aggregation FFF processes such as Selective Laser Sintering (SLS) and 3-D Printing (3DP) single-material parts are generated from thin slices of powder spread by compaction with a counter rotating roller. All aggregation FFF processes to date are lim-

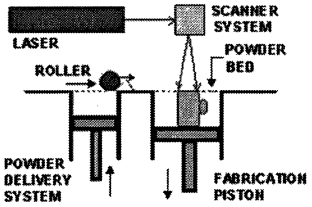

Figure 0.1 Working theory of SLS. Courtesy from Calstle Island's Worl Guide to Rapid Prototypings

ited to uniform build material by the powder laying itself. While we have recently seen the introduction of 3D-Color printing, to date, there are no processes allowing either material variation in the build, or control of factors such as porosity or composition. The ability to deposit powders selectively into a layer would represent a quantum leap advance for these processes.

In laser consolidation FFF processes, a part is built incrementally by pneumatic projection of powder grains into a small laser melt pool. Powder transport and deposition

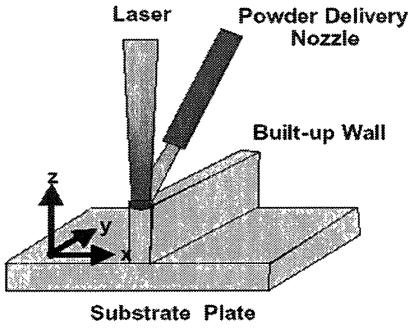

Figure 0.2 Laser consolidation process description, from Mould Makers Council Dinner meeting, January 25, 2001

remains a key process limitation. Accurate feed metering is difficult and alters the quality of the build material. Projection into the melt pool is notoriously inefficient, while unmelted powder grains cause a rough surface finish. The ability to accurately meter powder flowrates and deposit powder patterns would also represent a quantum advance in FFF which relies on the same specifications as for aggregation processes.

Powder feed control and deposition thus constitutes the ultimate objective of the research program to which the present work shall contribute.

0.2 Background of the vibratory micro L-valve

In a nutshell, a VMLV consists of a vertically vibrated horizontal micro-channel connected at one end to a powder reservoir, and at the other to a vertical delivery nozzle. This experimentally-designed VMLV was shown to be capable of repeatable dry powder flow-rate control from about 0.1 to $10 mm^3/s$ per mm^2 of nozzle cross-section using frequency modulation.

The VMLV was obtained by iteration through design of experiments [22] by Pegna et al. [27]. Although the VMLV had reached the proof of concept stages experimentally, there was no quantified understanding of why and how such device actually functions. Design of experiments has reached its limits in this instance and further advances in design and control of powder feed can only emerge from a detailed understanding of the physics underlying the device.

0.2.1 A brief on VMLV experimental design

Most fluidic transport systems for bulk material are designed for large flowrates, e.g: cement, grain, flour [25]. The few low flowrate gas transports that are used typically spray powders as the transport medium exits the nozzle and expands [43].

Flowrate modulation can be achieved only in a few instances, the most notable being the pneumatic L-Valve. Experimental design attempts at scaling down the pneumatic L-valve to the levels required for powder deposition in FFF failed [23].

A typical experimental L-valve is shown as Figure 0.3. An L-valve consists of silo con-

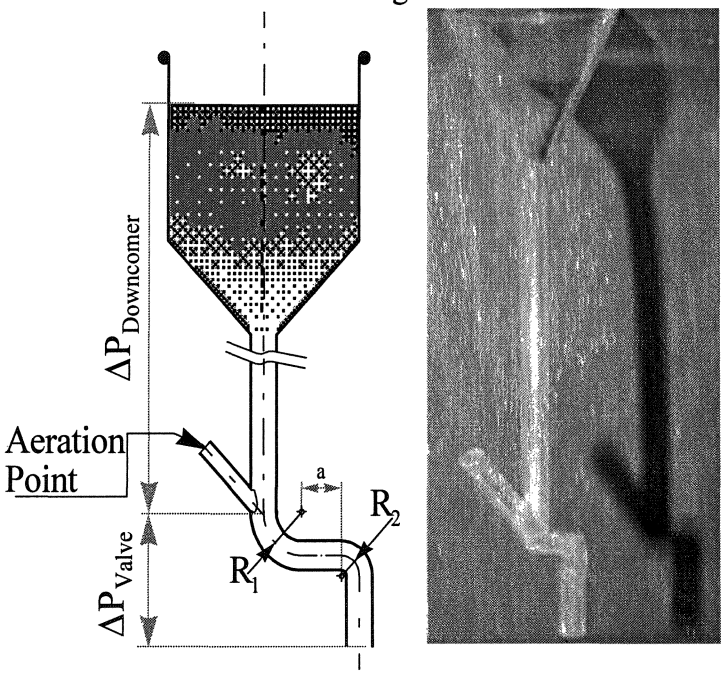

Figure 0.3 Sample experimental pneumatic L-Valve used in design of experiment (Figure courtesy of Pegna et al [23].)

nected to an elbowed downcomer. The elbow presents enough resistance to the flow that the creation of an angle of repose in the horizontal arm is sufficient to prevent flow. Injection of pressurized gas at the elbow fluidizes the powder, initiating a flow down the nozzle. Although some level of flow modulation can be achieved by adjusting the intake pressure, an L-Valve is first and foremost an on-off switch. Moreover, as the two-phase flow reaches the outlet, the gas expands spraying the powder. Typical flowrates in an

industrial L-valve are of the order of liters or cubic meter/second. Therefore, if the basic concept is attractive its implementation toward powder-based FFF is inconclusive.

An alternative to gas fluidization is vibration. This remark led Pegna et al. [23] to experiment with small L-valves that are vertically vibrated. A sample structures is shown in Figure 0.4. It was shown to be capable of modulating flowrates and depositing fine powder patterns.

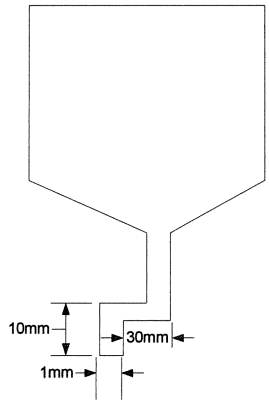

Figure 0.4 Sample experimental vibratory L-Valve (simplified drawing)

0.2.2 Position of the problem and further VMLV development

Development of VMLV to date was conducted through design of experiment. However, this process having reached its limits, modeling and experimental investigation have become necessary in order to develop an understanding of the physics underlying the VMLV. The present work shall contribute to further that understanding by examining the

process parameters driving the flow intensity through a vibrated horizontal micro-channel.

0.3 State of the art

0.3.1 Powder deposition

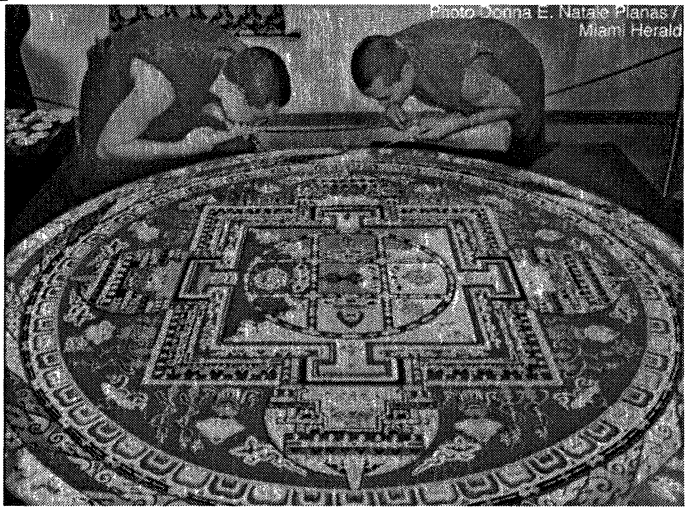

Figure 0.5 Sample Mandala decorative pattern illustrating size and complexity of feasible designs (Source: Miami Herald).

To our knowledge, the only prior art in matters of powder flow control and deposition is art literally. A journal and patent search only revealed a technological vacuum. This does not mean however that prior art is non existent, in fact powder deposition has been used for millenia as part of religious practices by Navajo indians and Tibetan monks. Both use manual hoppers to dispense powder patterns, often of large dimensions and in multiple layers. Figure 0.6 shows an example of such powder deposition patterns in Navajo sand painting. Other examples include Tibetan mandalas, such as the one shown in Figure 0.5.

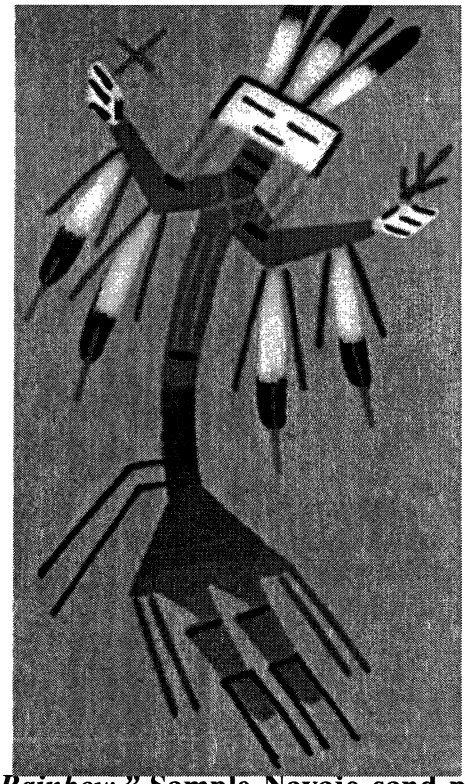

Figure 0.6 *"Rainbow,"* Sample Navajo sand painting by Shush Yellowhorse (private collection-Reproduced with permission).

0.3.2 Vibratory flow control of granular materials

Be it in the patent or journal literature, there are no references to dry powder flow control at low volumetric flowrates, or to the behavior of granular material in a horizontal micro-channel vibrated vertically. The only relevant bibliographical findings deal with the response of shallow powder beds to vibrations, often modeled after one particle bouncing off a vertically vibrated plate. Such approximation assumes the dominance of interactions between plate and particle over that among particles. The validity of this assumption is only tested in one experimental article.

0.4 Rationale

Given the lack of relevant literature, this project almost has to start from first principles. We therefore adopted a dual theoretical and experimental approach. The only ground upon which the theoretical analysis can proceed is the response of shallow beds to vertical vibrations. The experimental branch for its part, can only proceed from flowrate measurements given the difficulty of observerving the dynamic behavior of powder beds.

The plan of investigation to uncover the mechanisms governing powder flow thus consisted of first understanding the behavior of a particle bouncing off a vertically vibrated plate (refered to as "single plate problem"). After that, we further did some experimental work with the VMLV. We of course expect that there will be a gap between the behaviors of a single particle bouncing and that of a shallow powder flowing down that channel.

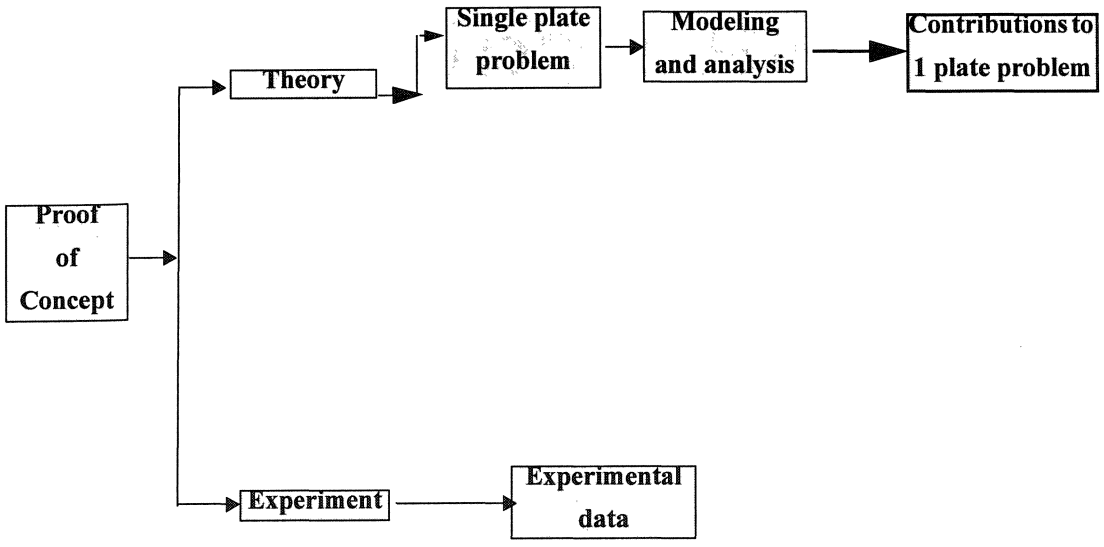

Figure 0.7 Map of the contributions

0.5 Organization of the manuscript

Following the plan of investigation exposed in Section 0.5, this manuscript proceeds to expose modeling and simulations in chapters 2. Experimental flow characterization is the subject of chapter 4. Conclusion draws a correlation between theory and experiments, and lays out a plan for further research.

0.5.1 Chapter 1

Few researchers have characterized the vibrational behavior of shallow powder beds by analysis and simulation[3][5][6]. Even fewer have pursued an experimental approach[7]. Simulations of vertical vibrations to date describe a phenomenon that is mostly chaotic in nature, though a few periodic, yet unstable, modes have been identified. Experimental results mostly agree, but also point out some unexplained singular modes with remarkable stability that our experiments confirmed. These modes can be explained if we assume that the laws of elastic collisions do not hold at very low impact velocities so that a minimum "quantum" of kinetic energy be exchanged between the particle and the vibrating plate. A new impact model that matches classical laws except when approaching a minimum impact velocity is introduced. This minor chink in the laws of elastic rebound has a profound effect on simulated behavior, which is akin to “loss of ergodicity” of Hamiltonian system under non-hamiltonian perturbation[21]. It forces particle motion from a chaotic state into discrete, yet complex, but finite "allowed states." Transition between states is akin to a random walk.

0.5.2 Chapter 2

With the exception of manual sand-painting, dry powder flows at very low mass flow-rates have never been achieved in industrial settings. A novel vibrationnally actuated micro L-Valve was shown to produce scalable flowrates within a fraction of milligram per second with rough uncalibrated WC powders. This article is concerned with the experimental flow characterization in a micro L-Valve. In general, three flow modes were identified when scanning in frequency at constant amplitude. In the first mode, no flow occurs until a trigger frequency is reached. The flowrate then ramps up, peaks and ramps down until it eventually stabilizes and remains constant in the last and third mode. The third mode was further investigated to test the stability of the flowrate. Experiments show that the flowrate remains independant of frequency in the third mode and is repeatable. The powder load in the shaker appears to have a noticeable influence only during a final emptying phase.

0.6 Summary of main contributions

Our work proceeds from a replication of prior results concerning the one plate problem. Our first aim in addressing this issue was to implement a robust numerical solution that would avoid numerical limitations exposed in prior works. This robust solution allowed to not only replication of the prior results, but to further the research and identify its shortcomings. One of the major limitation came from the model of elastic impact used in

prior works, which turns out to be inadequate to represent low velocity impacts. A new model was thus introduced which in turn drastically alters the observed results.

The major computational challenge in simulating the one plate problem lies in finding the smallest root of a rapidly oscillating transcendental-polynomial function.

$$P\cos(\omega t) = -\frac{1}{2}\cdot g\cdot(t-t_0)^2 + v_0\cdot(t-t_0) + h_0 \qquad \text{(EQ 1)}$$

Where t_0, v_0, h_0 are particle initial conditions while p, ω are the plate amplitude and angular velocity.

This problem is known to have no analytical solution and to resist numerical methods. It was a source of problems in some of the prior investigations. A robust simulation was derived from a novel symbolic computation that relied on an original combination of recursive Taylor expansions and root isolation methods.

Prior works on the single plate problem found the response to be chaotic, except for instances called period-n motions, where the particle exhibits a periodic pattern of n bounces[3]. Our novel approach was tested by reproducing previously published simulations. More importantly, the robustness of our computational approach led to the discovery of a new class of motions, called period-$_s n$. In a period-$_s n$ motion, the particle

exhibits a stable pattern of n bounces, then lands on the plate with matching velocity. The discovery of period-$_s n$ motions led to the realization that elastic models were not representive of the physics of low-velocity impacts. A further contribution was thus the introduction of a novel model whereby a minimum quantum of kinetic energy must be exchanged at each impact. This minute alterations of the laws of impact mechanics has far reaching ramifications. Instead of the chaotic behavior observed in prior works and confirmed by digital experiments, we found through digital experiments that after seemingly random bounces, the particle eventually settles in a complex period-$_s n$ motion. Moreover, for a given frequency and amplitude combination, only one periodic motion can exist on the plate.

Flowrate measurement experiments conducted with different micro L-valves by scanning frequencies at constant amplitude showed interesting results. At low frequencies, no powder flow was observed. As the frequency increased so did the flowrate until it peaked and went back down to eventually stabilize at a constant low flowrate at high frequencies.

CHAPTER 1

QUANTIZATION EFFECTS IN SHALLOW POWDER BED VIBRATIONS

1.1 Abstract

Vibrational behavior of granular materials is extremely complex and only partially understood. Simulations to date describe a phenomenon that is mostly chaotic in nature, though a few periodic, yet unstable, modes have been identified. Experimental results mostly agree, but also point out some unexplained singular modes with remarkable stability that our experiments confirmed. These modes can be explained if we assume that the laws of elastic collisions do not hold at very low impact velocities so that a minimum "quantum" of kinetic energy be exchanged between the particle and the vibrating plate. A new impact model that matches classical laws except when approaching a minimum impact velocity is introduced. The particle motion is forced from a chaotic state into discrete, yet complex, but finite "allowed states." Transition between states is akin to a random walk.

1.2 Introduction

Ever since it was first observed 170 years ago, the flow of vibrated granular materials have been widely studied [1][34][2][11]. It has attracted a number of researchers due to the very complex nature of the phenomena [1][10] as well as the practical applications [5][12][14]: the materials exposed to vibrations are sometimes used instead of the upward flow in fluidized bed reactors; to induce flow in devices such are hoppers and chutes, and

for segregation sizes, which all represent the cases of high material flows [1][5]. However, there is a number of other industrial applications (ranging from pharmaceuticals and packing to free form fabrication (FFF)), where the understanding of the small flows of powdered material is essential [1][13]. Since the granular state received the international recognition in 1992 [12] the need for understanding particles subject to vertical vibrations became even more apparent.

Several researchers have previously examined the behavior of a bed of particles subjected to vertical vibrations, relaying, for analytical purposes, on the similarity between the vertical oscillations of a shallow granular bed and that of a single particle bouncing elastically off a sinusoidally oscillating rigid plate [1][5][14]. This apparently simple model can be quite deceptive, as it exhibits an amazingly rich variety of behaviors presumed to be chaotic with occasional bifurcations, interspersed with families of periodic motions. Periodic motions identified in the literature consist of repeated patterns of one or more parabolic trajectories. The number n of successive parabolic trajectories before a pattern is repeated is used as a qualifier to characterize the motion, thus called *period-n motion*. When needed, the number k of plate periods needed to account for one period of the ball motion will be used as a subscript. For example Holmes [3] (figure 1.b) shows a period-2_2 motion consisting of a periodic succession of 2 parabolic trajectories over 2 plate periods. If multiple period-n_k motions are presumed to exist on the same k plate periods interval, we may have to refer to the order m of the motion as the order in which the first bounce occurs. If needed, this order will be indicated by a superscript period-n_k^m motion. For the most part, these period-n motions are surmised to be unstable.

Following a synopsis of published research, and a discussion of methods and results in light of our discoveries, this article identifies a new class of period-n motions where the last impact happens with zero relative velocity. Although the existence of stable orbits with long periods have been previously observed [2], to our knowledge, this class of phenomena has not been identified in the literature. Those periodical motions appear to constitute a fundamental pattern of behavior, which is at the core of our research on powder bed vibrations. We shall refer to these motions as *period-*$_s n$ motions, with appropriate subscripts and superscripts as needed to explicitly describe a period-$_s n_m^k$ motion. The "s" prefix subscript is meant to indicate "soft-landing." In a period-$_s n$ motion, the particle exhibits a series of zero or more elastic bounces before landing on the plate with matching velocity. The particle then rides on the plate until it is thrown off again and the pattern repeats. To illustrate the difference between period-n and period-$_s n$ one should compare Figure 1.1 to Holme's figure 1.b [3].

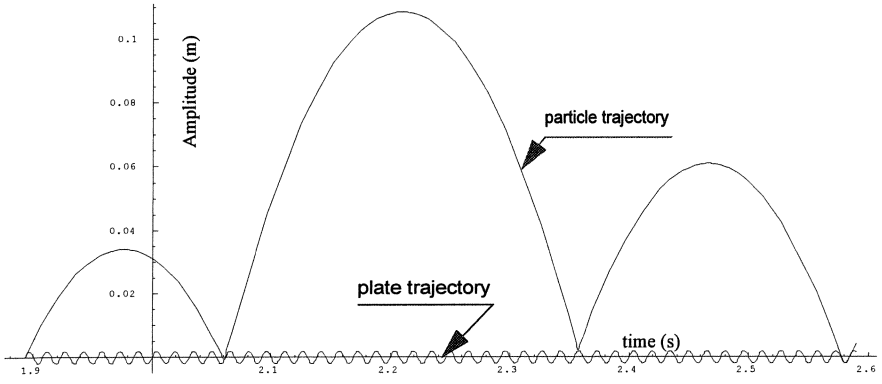

Figure1.1 Example of a period-$_s 4_{45}$ motion corresponding to the pattern detailed in Figure 1.13. (Amplitude: 2mm, frequency: 65Hz, coefficient of restitution: 0.5.)

The defining characteristic of period-$_{s}^{n}$ motions is their terminal zero relative velocity landing before being re-launched at a well-defined phase of the plate oscillation. Such low velocity impact however, fails to be adequately represented by existing models of elastic collision. Indeed such model is but an approximation as it is well known that a ball bouncing off the floor will not keep bouncing forever, even in the absence of air. As common sense experience indicates, a ball will fail to bounce back when dropped from below a certain height. The consideration that a minimum amount of kinetic energy needs to be exchanged between colliding bodies —or equivalently, that a minimum relative velocity is required for rebound— leads to a new collision model relating incoming and outgoing velocities. Interestingly, this approach leads to an equation for velocity transformation that is very similar to that of relativistic velocity transformation. Like its relativistic counterpart, which closely represents Galilean kinematics up to nearly the speed of light, our new model is nearly identical to existing elastic collision models until the impact velocity becomes almost as small as the critical minimum required for rebound.

This apparently benign modification of the laws governing elastic collisions has a profound effect on the problem at hand. Indeed, the state of each bounce can be represented by two variables that are initial position and particle velocity, or equivalently initial plate acceleration and particle velocity. Successive impacts can thus be represented by a series of points in the plane. Under the classical assumption of elastic impact, representative points for successive bounces form a cloud covering region of the plane. Under the resulting chaotic assumption, any velocity-acceleration combination is likely to happen. In con-

trast, when the new model for low-velocity impact is taken into account, it forces a quantization of the allowed states. For a given amplitude and frequency combination, only one pattern of discrete states is allowed. Representative points for successive bounces form a discrete and finite collection. This quantization effect can be understood as the effect of the new model expanding the soft landing conditions from a single phase to a continuous range. This will effectively allow the steady state pattern to occur after a series of apparently random transitional bounces. As soon as the particle impacts the plate with a low enough relative velocity, it will be captured by the plate and launched back at a precise phase corresponding to the plate deceleration greater than g. This will effectively lock the particle into a pattern of rebounds that will repeat ad-infinitum. Moreover, a perturbation of the particle motion will either have no effect, or will result in an apparently random pattern of bounces eventually returning to the stable pattern of allowed states. A perturbation of the plate motion will either have no effect if the non-dimensional acceleration is preserved, or will force the particle into a new "allowed state."

If such a minor chink in the constitutive laws of elastic collision does indeed exist, its consequences on the quantization of a bouncing particle should be noticeable by careful observation. To this end a series of experiments are to be conducted in which a spherical bead bounces off an oscillating platform. The experiment and its results however are outside the scope of this paper.

1.3 Review and discussion of prior works

The response of granular materials subjected to vertical vibrations has been studied previously [3][5][6], however the investigations of vibrational response of shallow powder beds are fairly limited [1].

This review has a two pronged objective. First, we intend to draw an objective portrait of the state of the art, this will be the topic of Section 1.3.2. Second, our theoretical and experimental advances enable us to revisit prior works and evaluate their methods, assumptions, and results. These remarks will be consigned in Section 1.3.3. Prior to that however, it is advisable to put some order in the presentation of the main concepts and notations. The formulation of the problem is rather trivial, though its solution is not. However each author uses a different notation and formalism which makes it difficult to compare all publications on an equal footing. In order to compare objectively all works and insert our contribution as well, we shall start in Section 1.3.1 with an introduction of the topic and the notations used in modeling it.

1.3.1 Notation

In this section, we introduce the notation that will be used throughout this article. This early introduction will allow us to cover the existing body of prior works in a uniform and consistent manner. Although notations and graphical representations used here to discuss

prior works may be different from the original, every effort was made to preserve the intended meaning.

Representation of the plate kinematics: Let $z_{P/G}(t)$, $z'_{P/G}(t)$, and $z''_{P/G}(t)$ respectively represent the plate elongation, velocity, and acceleration along the vertical axis measured in the ground frame. Without loss of generality, we can represent the oscillatory motion of the plate by a cosine function of amplitude P and pulsation ω (or equivalently period $T = \frac{2\pi}{\omega}$.)

$$z_{P/G}(t) = P\cos(\omega t) \quad . \tag{EQ 1}$$

It will be useful for the rest of this argument to write the first and second derivatives in forms that eliminate time:

$$z'_{P/G}(t) = -P\omega\sin(\omega t) = \pm\omega\sqrt{P^2 - z_{P/G}^2} \tag{EQ 2}$$

$$z''_{P/G}(t) = -P\omega^2\cos(\omega t) = -\omega^2 z_{P/G} \quad . \tag{EQ 3}$$

A few researchers have characterized the motion in terms of non-dimensional parameters. This is also the convention we shall adopt in this article whenever applicable. Letting g stand for the acceleration of gravity, the non-dimensional position, velocity and accelerations are respectively defined as:

$$\xi_{P/G}(t) = \frac{z_{P/G}(t)}{P} = \cos(\omega t) \quad , \tag{EQ 4}$$

$$\xi'_{P/G}(t) = \frac{z'_{P/G}(t)}{P\omega} = \pm\sqrt{1-\xi^2_{P/G}(t)} \quad , \tag{EQ 5}$$

$$\xi''_{P/G}(t) = \frac{z''_{P}(t)}{g} = -\frac{P\omega^2}{g}\xi_{P/G} \quad . \tag{EQ 6}$$

An important parameter in this and other articles is the non-dimensional acceleration γ:

$$\gamma = \frac{P\omega^2}{g} \quad . \tag{EQ 7}$$

Representation of the particle kinematics: In this article, we shall denote by $z_{B/G}$ and $z_{B/P}$ respectively the particle position relative to the ground and plate frames. The corresponding velocities and accelerations will be denoted by $z'_{B/G}$, $z'_{B/P}$, $z''_{B/G}$ and $z''_{B/P}$. In order to be consistent with the rest of the literature, we also define the non-dimensional counterpart to these entities as:

$$\xi_{B/G} = \frac{z_{B/G}}{P}, \quad \xi_{B/P} = \frac{z_{B/P}}{P} \quad , \tag{EQ 8}$$

$$\xi'_{B/G} = \frac{z'_{B/G}}{P\omega}, \quad \xi'_{B/P} = \frac{z'_{B/P}}{P\omega} \quad , \tag{EQ 9}$$

$$\xi''_{B/G} = \frac{z''_{B/G}}{g} \text{, and} \quad \xi''_{B/P} = \frac{z''_{B/P}}{g} \quad . \tag{EQ 10}$$

Representation of impact kinetics: All published articles consider the plate to be perfectly rigid and of large mass. In effect, this hypothesis allows us to consider the plate motion to be unaffected by the particle impact. The relation between incoming and outgo-

ing relative velocities is thus governed by the law of elastic impact with a coefficient of restitution η . Let us denote by ${}_{i}t$ the time of the i^{th} impact. As a lexicographic rule, whenever a function f of time is expressed at ${}_{i}t$, we shall use the following shorthand:

$$ {}_{i}f = f({}_{i}t) \quad . \tag{EQ 11}$$

The time of flight interval between the $(i\text{-}1)^{th}$ and the i^{th} impacts will be denoted by ${}_{i}\tau$:

$$ {}_{i}\tau = {}_{i}t - {}_{(i-1)}t \quad . \tag{EQ 12}$$

The incoming and outgoing velocities at the i^{th} impact will be denoted respectively with a "-" or "+" prefix superscript. The law governing the velocity transformation relative to the plate is thus:

$$ {}^{+}_{i}z'_{B/P} = -\eta \; {}^{-}_{i}z'_{B/P} \tag{EQ 13}$$

or equivalently

$$ {}^{+}_{i}\xi'_{B/P} = -\eta \; {}^{-}_{i}\xi'_{B/P} \quad . \tag{EQ 14}$$

These relations expressed by (EQ 13) and (EQ 14) in the ground reference frame become:

$$ {}^{+}_{i}z'_{B/G} = -\eta \; {}^{-}_{i}z'_{B/P} + (1+\eta) \; {}_{i}z'_{P/G} \quad ; \tag{EQ 15}$$

which, when expressed in non-dimensional form becomes:

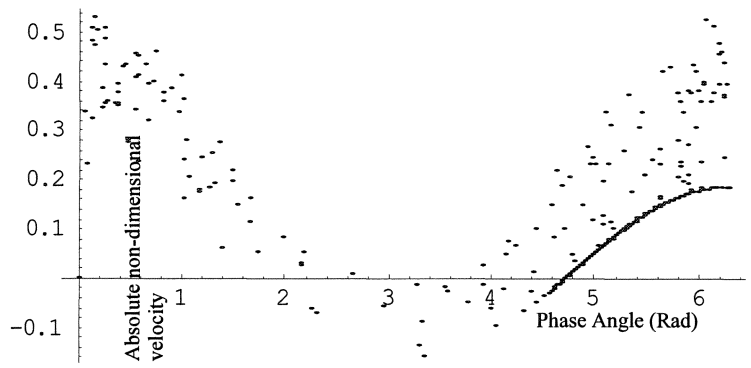

Figure 1.2 Example of Poincaré diagram.

$$\overset{+}{i}\xi'_{B/G} = -\eta\ \overset{-}{i}\xi'_{B/P} + (1+\eta)\ {}_{i}\xi'_{P/G} \qquad \text{(EQ 16)}$$

Poincaré Diagrams. Each bounce can be represented by two variables, initial phase (or equivalently initial plate acceleration, or initial particle position) and velocity. This leads to a representation of the particle motion as a series of representative points in the plane, called a *Poincaré diagram* [50]. Under classical models of chaotic behavior the Poincaré diagram will appear as a cloud of points covering an area of the plane. This phenomenon is illustrated in Figure 1.2, which records the first 300 bounces of a particle dropped from a 2 cm height onto a plate vibrating at 68 Hertz with a 2mm amplitude.Each point represents the phase angle and absolute non-dimensional velocity associated with each impact of a particle dropped from a height of 2 cm onto a plate vibrating at 68Hz with 2mm amplitude.

1.3.2 Literature survey

Granular materials exhibit a wide range of unusual behaviors and as such, have been subjected to a number of investigations [1][6][11]-[52]. As collisions of particles in a granular material are inelastic, these systems are intristically dissipative [5][12]. It is very difficult to measure experimentally the distribution, density and velocity of the particles inside the system and therefore, most of the researchers in the field used analytical approach or computer simulation [3][4][5][13][17]. Experimental research papers mainly focused on external measurements of macroscopic parameters such as the dispersion relation or pressure fluctuations on the bottom of the plate [17]-[20]. Geminard and Laroche [12] investigated energy of the single bead bouncing on a single vibrating plate, in both experimental and numerical simulations. As our work is primarily concerned with shallow beds, the following review will be even more selective, highlighting the major theoretical approaches, and the one experimental work relevant to ours [9].

Analysis and simulation: The seminal works in this field can be traced back to Wood and Byrne [4], who established the impact governing equation (EQ 15), and Holmes [3] who proposed an analytical solution. In order to solve the rather complex computational problem formulated by Wood and Byrne [4], Holmes [3] introduced a simplifying assumption by neglecting the plate position in computing the time of flight. In effect, only the plate velocity is accounted for in computing the rebound. Under this assumption, the time of flight becomes that of a particle in free fall departing from the plate's average

position with a velocity imparted by the rebound. Hence the time of flight was given by the following equation:

$$(i+1)^{\tau} = 2\frac{\dot{z}^{i}\,\mathrm{B/G}}{g} \qquad \text{(EQ 17)}$$

Although this simple approximation allows to solve for velocity transformation from one impact to the next, the phenomenon still remains highly complex, exhibiting irregular non-periodic solutions, as well as harmonic and sub-harmonic responses. In order to conduct a computationally tractable stability analysis, Holmes [3] further assumes that the collision is perfectly elastic (coefficient of restitution e=1.) Under these conditions, Holmes [3] identifies transition from harmonic to stochastic responses. It is interesting to note that the patterns of responses are qualitatively similar to those obtained by other researchers, including ourselves, who did not resort to Holmes's simplifying assumptions. The appropriateness of these assumptions and their results will be subjected to a critical analysis in our forthcoming discussion in Section 1.3.3.

Another analytical investigation of this phenomenon by means of simulations is due to Hjelmfelt [5]. In contrast to Holmes[3], Hjemfelt did not resort to a simplified kinematics but used iterative marching methods to detect impacts between plate and particle. In this case the author points out that his approach is more representative of the actual physics of the phenomenon. In particular, Holmes model can occasionally produce negative rebound velocities. Such negative rebound velocities are perfectly valid physical solutions that can

be handled by Hjemfelt, but are not compatible with Holme's assumption since the particle would find itself below the table. Numerical experiments were conducted by Hjelmfelt with a coefficient of restitution of 0.4 and focus on a range of non-dimensional acceleration $0 \leq \gamma \leq 10$. These values are the same as used for simulation in prior works.

Hjelmfelt [5] did not identify any of the periodic motions stressed by other researchers. Yet, and despite using a different approach than Holmes [3], he eventually confirmed qualitatively a number of characteristics from prior studies with estimated measures of stability. Simulations show regions of transition to chaotic behavior, which are qualified by experimental estimation of their associated Lyapunov exponents.

The latest instance of simulated behavior studies is due to Luo and Han [6] who focused on period-1 motions and their stability. In essence, the conditions for period-1 motions identified by Luo and Han [6] reduce to Holmes [3] in the case of perfectly elastic impacts ($\eta = 1$.) For non-elastic collision, Luo and Han [6] formulate a closed form expression of Eigenvalues of the differential mapping between impacts. With a few exceptions, periodic motions are shown to be instable.

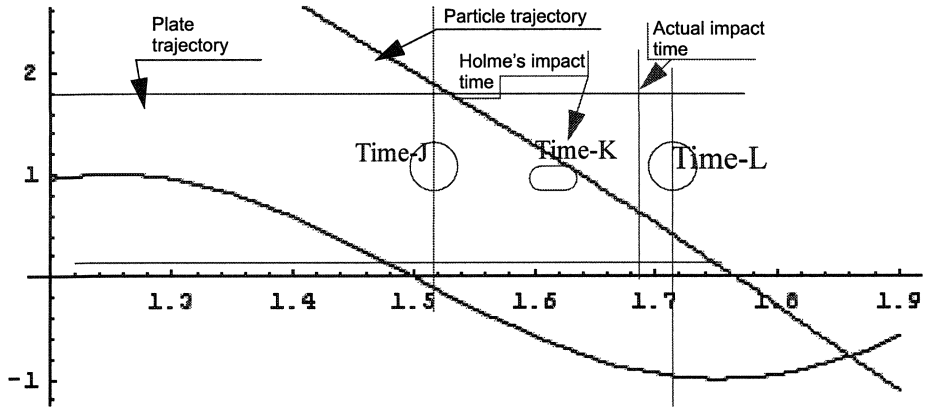

Figure 1.3 The impact between the particle and the plate must occur during the interval when the particle trajectory intersects the plate's range of motion.

Experimental investigations:. Our only reference on this matters is Brennen et al. [7]. This article provides a good overview of prior research, and the results of their original experiment concurs with other reports as well as our own. Brennen et al.'s setup uses a transparent rectangular box filled with shallow beds of $\varnothing 2.85$ mm spherical beads. The size of the beads allow them to neglect the effect of interstitial air flows. To observe the dynamic behavior of the bed, Brennen et al. top the bed with a light weight lid, and observe the bed expansion under a stroboscope.

The main remark from this experiment is that no significant expansion occurs for values of the non-dimensional acceleration γ between 1 and 2. Observations during this phase indicate that the flight time of the beads is less than 0.6 period and that the particles are riding on the plate for the rest of their periodic motion. Then at value of γ near 2, the bed experiences a sudden expansion, expanding gradually further afterward. In order to

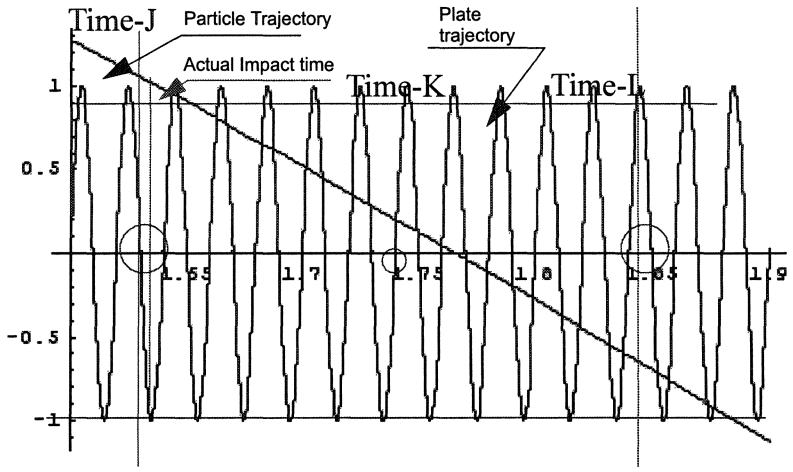

Figure 1.4 For the same conditions as in Figure 1.3, but shorter period, the impact time and velocity are altered significantly.

explain this phenomenon Brennen et al. surmise that the particles experience a period-1 motion. Using Holme's [3] expression for the period-1 non-dimensional acceleration, Brennen infers a coefficient of restitution of the order of 0.25 for such motion to occur.

1.3.3 Discussion

Assessment of Holmes model: Holmes [3] contribution rests on the approximation that the plate elongation does not affect significantly the impact time and rebound velocity. This approximation holds exactly in the case of period-1 motion since impact always occur at the same phase angle of plate displacement. In this case the work of Holmes[3] rejoins that of Luo and Han [6]. In most circumstances however our results concur with earlier criticisms by Luo and Han [6] concerning the appropriateness of Holme's approximation. First, we found that Holme's only holds when the plate period is large compared

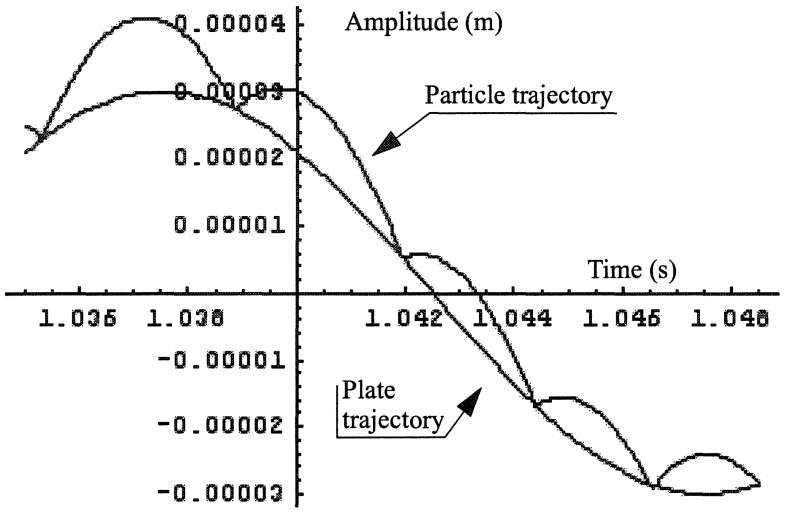

Figure 1.5 When the particle time of flight is short with respect to the period, Holmes approximation fails to capture the phenomenon accurately.

to the particle travel time through the plate trajectory. Second, Holmes approximation requires that the particle velocity reverse course after impact, this often is not the case as judicially pointed by Luo and Han [6]. Finally, we repeated Holmes experiments and found that the assumption affects the Poincaré distribution. Yet, the qualitative results obtained by Holmes are strikingly similar to ours; most notably the horseshoe pattern of the Poincaré diagram and the existence of strange attractors.

The first count is illustrated by figures 1.3 and 1.4. They show that Holmes assumption does not hold when the particle transit through the plate's range of motion lasts more than a period. Another instance where Holmes approximation fails to capture the phenomenon is when the period is much longer than the time of flight. This is illustrated by figure 1.5.

The second point was already discussed by other researchers [5] and is illustrated by Figure 1.12.

The third point concerning impact distribution is an original finding of our research that is illustrated further on in this article when we discuss strange attractors and point distribution in Section 1.6. Whereas Holmes' approximation yields a nearly uniform distribution of Poincaré points, our model shows an accumulation near phase zero (modulo 2π.) This result is illustrated in figures 1.10 and 1.11.

Periodic motion and stability conditions in Holmes [3] and Luo and Han [6]: To our knowledge, all prior works consider only elastic impact, regardless of approximation used. In all instances, the elastic impact assumption leads to chaotic models with occasional domains where the motion becomes periodic. Having identified such periodic modes, a few authors have sought to characterize their stability. Typically periodic modes are identified through fixed points $(\bar{\varphi}, \bar{V})$ of the mapping $(\varphi_{i+1}, v_{i+1}) = f(\varphi_i, v_i)$ yielding phase angle φ_{i+1} and velocity v_{i+1} from the prior bounce conditions.

$$f(\bar{\phi}, \bar{V}) = (\bar{\phi}, \bar{V}) \qquad \text{(EQ 18)}$$

As rightfully pointed out by Holmes [3] focusing on fixed points alone will only yield period-1 motions. Other periodic modes may exist, however, when the motion cycles through a series of n points, thus experiencing period-n motion. Holmes approximation allowed him to develop a recursive formulation relating the bounces. However, Holmes

and other researchers that followed him failed to capture the conditions for period-n motion. Period-n motion occur when the representative point on the Poincaré diagram cycles through n points. Hence, in order to characterize such period-n motion, one must identify the fixed point of an n-dimensional mapping. Below is an original finding of our research that formulates this fixed point in terms of Holmes approximation. Letting X_i represent n successive bounces on the Poincaré diagram,

$$X_i = \begin{bmatrix} \varphi_{i+n-1} \\ v_{i+n-1} \\ \varphi_{i+n-2} \\ v_{i+n-2} \\ .... \\ \varphi_i \\ v_i \end{bmatrix} , \qquad \text{(EQ 19)}$$

the fixed points of the n-dimensional mapping corresponding to period-n motions must satisfy the following equation, which is obtained by applying the mapping and rotating the points:

$$X_{i+1} = \begin{bmatrix} \varphi_i + v_i \\ \gamma v_i - \alpha\cos(\varphi_i + v_i) \\ \varphi_{i+n-1} + v_{i+n-1} \\ \gamma v_{i+n-1} - \alpha\cos(\varphi_{i+n-1} + v_{i+n-1}) \\ \varphi_{i+n-2} + v_{i+n-2} \\ \gamma v_{i+n-2} - \alpha\cos(\varphi_{i+n-2} + v_{i+n-2}) \\ \gamma v_i - \alpha\cos(\varphi_i + v_i) \\ \cdots \\ \varphi_{i+1} + v_{i+1} \\ \gamma v_{i+1} - \alpha\cos(\varphi_{i+1} + v_{i+1}) \end{bmatrix} = X_i = \begin{bmatrix} \varphi_{i+n-1} \\ v_{i+n-1} \\ \varphi_{i+n-2} \\ v_{i+n-2} \\ \cdots \\ \varphi_i \\ v_i \end{bmatrix} .$$

(EQ 20)

Unfortunately, as we saw earlier, Holmes approximation fails to adequately model but periodic motions that all land at a same plate height. For practical purposes, this limit Holmes to period-1 motions.

Armed with a fixed point formulation that characterizes period-n motions, one can now address the issue of stability of such periodic modes by studying the Jacobian of the mapping. This is what was achieved by Holmes [3] and by Luo and Han [6] for respectively approximated and numerically simulated period-1 motions. A corresponding stability analysis for period-n would require a similar analysis on the Jacobian of the mapping (EQ 20) for Holmes, or a numerical equivalent for Luo and Han.

Compared to our research, the results of Holmes [3] and Luo and Han [6] appear to be an artifact of the elastic model. With the low velocity impact model that we introduce in Section 1.5, period-$_s$n motions are a necessary outcome.

Observations of chaotic behavior by Hjelmfelt [5]: Hjelmfelt's research occupies a unique position in the field for its extensive analysis of chaos, using numerical simulation to estimate the Lyapunov exponent of the mapping. Without going into the numerical estimation of Lyapunov exponent, we repeated Hjelmfelt's experiments and compared his conclusions to ours.

Hjelmfelt's simulation [5] concurred with prior observations of strange attractors by Holmes [3], without resorting to approximations. He observed the phenomenon of the bounces being attenuated during plate downswing and the motion dying out on the plate upswing. This observation also concurs with ours, as Hjelmfelt's figure 1 should be compared to our Figure 1.12.

In plotting the non-dimensional impact velocities versus non-dimensional acceleration, Hjelmfelt [5] identified downward parabolic shaped patterns that were assumed to be artifacts of the phenomenon. Our implementation of Hjelmfelt's approach [9], illustrated in Figure 1.6, found these patterns to be characteristic of the initial conditions, and not of the ensuing chaotic behavior. Our simulation reproduced the patterns observed by Hjelmfelt [5], even when the low velocity impact model introduced in Section 1.5 is used. The same parabolic patterns are observed corresponding to the first bounce off the plate.

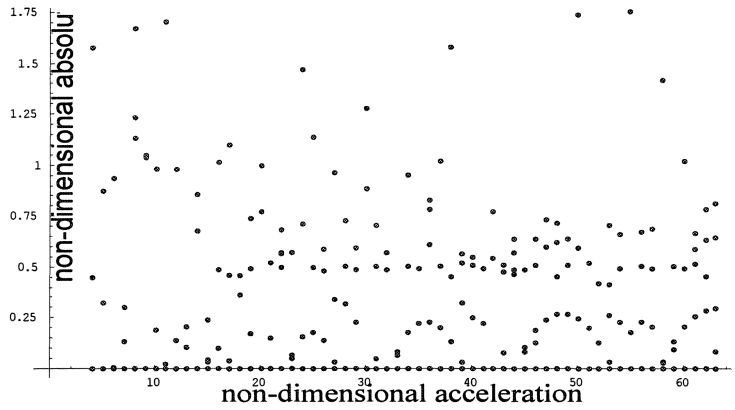

Figure 1.6 The graph shows the same characteristic downward parabolic pattern as Hjelmfelt [5], which we found to be an artifact of initial conditions.

1.4 Periodic response with soft landing

Experiments indicate that amongst the apparently chaotic motion of a particle bouncing on a vibrating plate, there are small regions that are well-behaved with characteristically higher jumps. This can be explained in first approximation if we consider the case of a ball at rest on the plate at the origin. In such a case, if the plate's downward acceleration was ever to decrease below -g, then the plate and particle would separate, with the ball continuing on a parabolic trajectory in the ground frame until the next impact. This case is illustrated by Figure 1.7

Particle initially at rest on a vibrating plate: Using the non-dimensional notation introduced in Section 1.3.1, let us consider the initial condition of a particle riding on the plate.

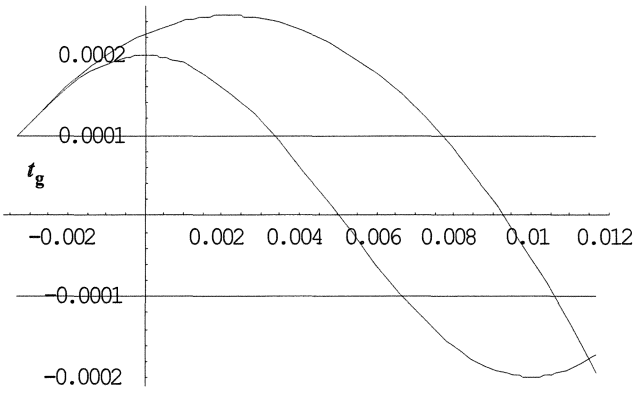

Figure 1.7 Illustration of the case where the particle is initially at rest on a vibrating plate.

As illustrated in Figure 1.7, particle and plate trajectories will separate when the plate's non-dimensional acceleration reaches -1; at which point the plate must have respective height and velocity:

$$ {}_g\xi = \frac{1}{\gamma} \quad \text{, and} \quad {}_g\xi' = \sqrt{1 - \frac{1}{\gamma^2}} \quad . \qquad \text{(EQ 21)} $$

The time at which this separation will happen is during the upward motion of the plate, that is at time

$$ {}_gt = \frac{1}{\omega}(-\operatorname{acos}({}_g\xi) + 2n\pi) \qquad n \in Z. \qquad \text{(EQ 22)} $$

From this time and until the next impact, the particle then follows a parabolic trajectory with non-dimensional position and velocity respectively equal to:

$$\xi_{B/G}(t) = -\frac{1}{2}\cdot\frac{\omega^2}{\gamma}(t-{}_g t)^2 + \omega\cdot{}_g\xi'(t-{}_g t)+\frac{1}{\gamma} \quad , \tag{EQ 23}$$

$$\xi'_{B/G}(t) = -\frac{\omega}{\gamma}(t-{}_g t)+{}_g\xi' \tag{EQ 24}$$

The particle will reach its maximum height at time:

$${}_h t = \frac{\gamma}{\omega}\cdot{}_g\xi'+{}_g t \quad , \tag{EQ 25}$$

where the height is then:

$$\xi_{B/G}({}_h t) = \frac{\gamma}{2}\cdot{}_g\xi'^2+{}_g\xi \tag{EQ 26}$$

Boundary conditions so no bounce will occur: The case studied above will, in most circumstances lead to the particle bouncing chaotically off the plate. There are however, instances where the particle will land on the plate with matching velocity, hence its motion will not be governed by the laws governing elastic impact. Rather, the ball will lift from the plate, follow a parabolic trajectory and meet the plate again at the only place where velocities can match, that is when the plate is at height ${}_g\xi$ during its downswing. Assuming, without loss of generality, that the particle separates from the plate at time

$${}_g t = -\frac{1}{\omega}\text{acos}({}_g\xi) \quad , \tag{EQ 27}$$

then the particle may only land at times

$$_{l}t = \frac{1}{\omega}(\text{acos}(_{g}\xi) + 2n\pi) \quad , n = 0, 1, 2,... \tag{EQ 28}$$

or equivalently

$$_{l}t = -_{g}t + nT \quad . \tag{EQ 29}$$

From time $_{l}t$ until $_{g}t' = _{l}t + 2_{g}t + T$ the particle will then be stationary on the plate. Then at time $_{g}t'$ it will lift again from the plate and follow the same parabolic trajectory as before. We can see therefore that the particle will then adopt a periodic motion composed a section of free fall and a section of vibratory motion. The period of the particle's motion is thus a multiple of the plate's period.

$$_{B}T = (n + 1)T, n = 0, 1, 2,... \tag{EQ 30}$$

Classes of parabolic trajectories meeting boundary conditions: In order not to experience an elastic impact, the particle must terminate its parabolic trajectory with matching plate position and velocity.

Given that the particle time of flight to return to altitude $_{g}\xi$ with velocity $-_{g}\xi'$ is:

$$_{g}\tau = 2\omega\gamma \cdot _{g}\xi' \quad , \tag{EQ 31}$$

it must be that $_{g}\tau$ corresponds to the time interval between $_{g}t$ and $_{l}t$.

$$ {}_{g}\tau = -2 \cdot {}_{g}t + nT \qquad \text{(EQ 32)} $$

Given that ${}_{g}\tau$ and ${}_{g}t$ have explicit definitions in terms of the plate kinematics ((EQ 31) and (EQ 27) respectively) we can establish a relation between plate amplitude and frequency:

$$ 2\omega\gamma \cdot {}_{g}\xi' = \frac{2}{\omega}\operatorname{acos}\left(\frac{1}{\gamma}\right) + 2n\frac{\pi}{\omega} \quad . \qquad \text{(EQ 33)} $$

Using (EQ 21) to eliminate ${}_{g}\xi'$ we find that the plate amplitude and frequency must satisfy the following relation:

$$ \sqrt{\gamma^2 - 1} - \operatorname{acos}\left(\frac{1}{\gamma}\right) = n\pi \qquad \text{(EQ 34)} $$

Note that the first four roots of (EQ 34) are 1, 4.60334, 7.78971, and 10.9499. After that the roots become large enough that we can approximate $\sqrt{\gamma^2 - 1}$ and $\operatorname{acos}\left(\frac{1}{\gamma}\right)$ with γ and $\frac{\pi}{2}$ respectively so the roots become uniformly spaced in first approximation:

$$ \gamma \approx n\pi - \frac{\pi}{2} \quad , (n>5.) \qquad \text{(EQ 35)} $$

At this venue, it is important to note that period-${}_{s}n$ phenomena are purely kinematic and independent of the coefficient of restitution η, as opposed to period-n motions identified by Holmes [3] and Luo et al. [6].

Conclusion: It is known that the problem of a particle bouncing elastically off a plate in sinusoidal motion will be mostly chaotic. However, we have found that there exist domains in which, there will be a definite well-behaved response. The mode at which such response will occur are such that the non-dimensional acceleration is a solution of (EQ 34).

Example 1: Consider a plate vibrating at 50Hz (Pulsation $\omega = 100\pi$ radian/second). The corresponding first five amplitudes that will lead to the ball bouncing off the plate in singular mode are: 0.099, 0.457, 0.774, 1.088, 1.401 mm. The height z_g at which the particle and plate separate is the same for all amplitudes, in accordance with (EQ 21). For a frequency of 50Hz, the value of z_g is 0.099 mm. Note that this is the same as the first mode amplitude, meaning that the parabolic arc reduces to a point which is the crest of the sine wave. Modes 2, 3, and 4 are shown in Figure 1.8. However, those solutions are not stable since as soon as the relative velocity between particle and plate becomes non-zero (because of perturbation), the particle will not be able to rest on plate anymore.

Example 2: We consider now the case of a constant amplitude vibration of magnitude P = 0.00077 meters(to allow the periodical states at 50Hz). The corresponding first five frequencies that will lead to the particle bouncing off the plate in singular mode are 17.9147,

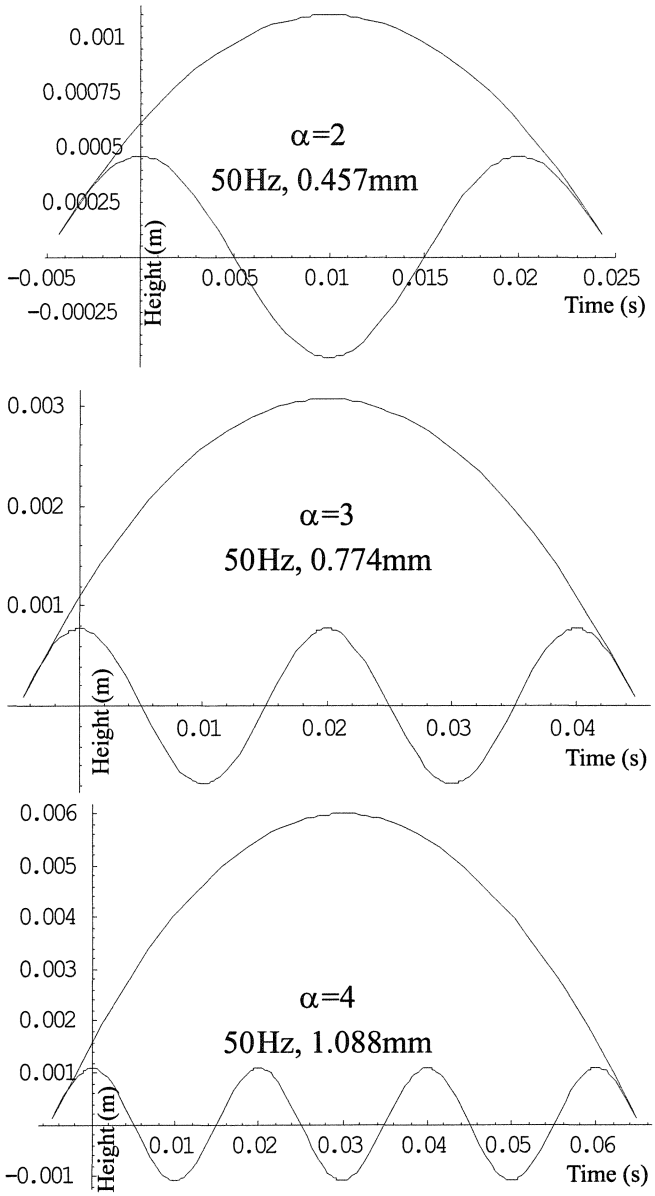

Figure 1.8 Illustration of the second, third and fourth singular mode at 50 Hz.

38.4367, 50., 59.2808, and 67.2737 Hertz. Note that as before the first mode consists only of the crest of the sine wave. Modes 2, 3, and 4 are shown in Figure 1.9.

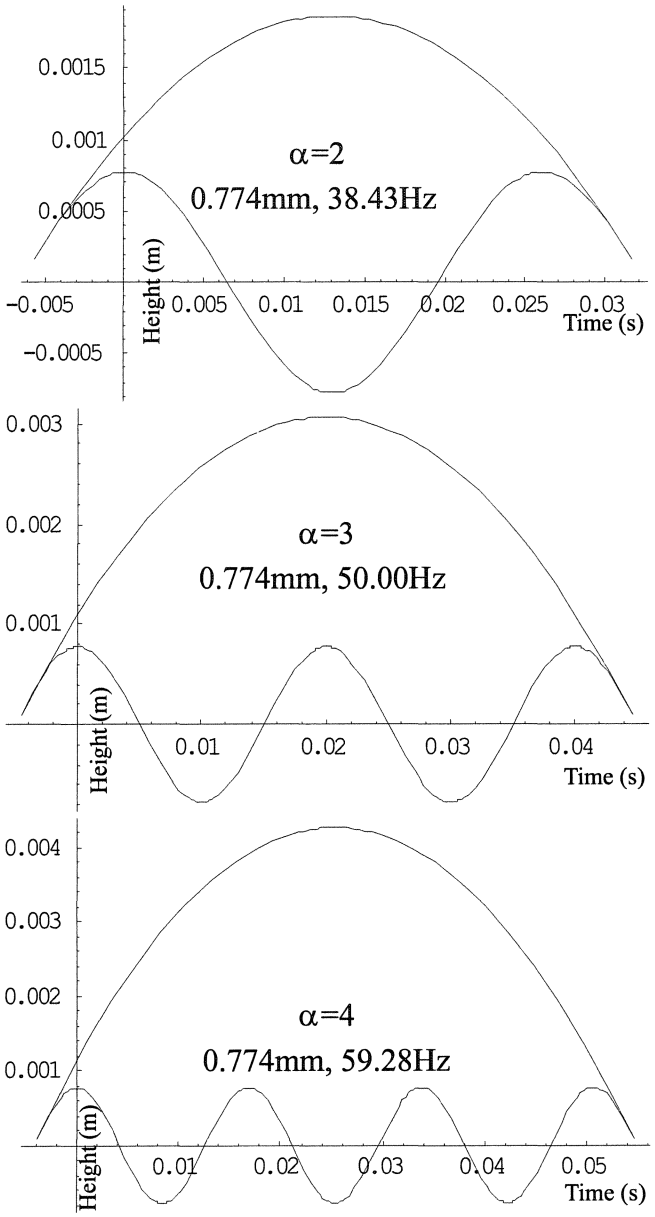

Figure 1.9 Illustration of the second, third and fourth singular mode for constant amplitude of 0.774 mm.

1.5 Low velocity impact model

The typical model of elastic impact considers only kinetic losses proportional to the velocity. Letting $\overset{-}{v}$ and $\overset{+}{v}$ stand respectively for incoming and outgoing impact velocities, the elastic model translates into the well known formula:

$$\overset{+}{v} = -\eta \cdot \overset{-}{v} \qquad \text{(EQ 36)}$$

This model is problematic however when the impact velocity becomes small and the kinetic energy assumed to be dissipated decreases without ever reaching zero. This model dictates that, contrary to experience, a particle bouncing elastically on a fixed plate will continue to bounce ad infinitum without ever coming to rest.

In practice, however, we know that independent to the elasticity of the materials involved, a spherical object left to fall freely will not bounce back if dropped from below a certain height $\underset{\sim}{h}$. Letting m stand for the mass of the particle, the height $\underset{\sim}{h}$ gives us a measure of the minimum energy $\underset{\sim}{\varepsilon}$ dissipated in the impact:

$$\underset{\sim}{\varepsilon} = mg\underset{\sim}{h} \qquad \text{(EQ 37)}$$

Equivalently, this experiment dictates the minimum impact velocity $\underset{\sim}{v}$ required for elastic bounce:

$$\underset{\sim}{v} = \sqrt{2g\underset{\sim}{h}} \quad . \tag{EQ 38}$$

For low velocity impact, we shall therefore consider that part of the kinetic energy corresponding to

$$\underset{\sim}{\varepsilon} = \frac{1}{2}m\underset{\sim}{v}^2 \tag{EQ 39}$$

is lost before the elastic bounce can even occur. In addition to incoming and outgoing velocities ^{-}v and ^{+}v, we now need to introduce the equivalent incoming velocity ^{0}v after $\underset{\sim}{\varepsilon}$ of the incoming kinetic energy is dissipated. We can relate ^{0}v to ^{-}v through a simple energy balance:

$$\begin{cases} {}^{0}v = {}^{-}v\sqrt{1-\left(\dfrac{\underset{\sim}{v}}{{}^{-}v}\right)^2}, & {}^{-}v \geq \underset{\sim}{v} \\ {}^{0}v = 0, & {}^{-}v < \underset{\sim}{v} \end{cases} \tag{EQ 40}$$

Note the similarity of this law to that governing coordinate transforms in special relativity. Just like it, it will reduce to $^{0}v \approx {}^{-}v$ in most instances. The incoming velocity ^{-}v will have to come within twice of $\underset{\sim}{v}$ to even have a 10% influence on v^{o}. Nevertheless, it is an effect that we must account for if we are to model all possible instances of a particle bouncing on a vibrating plate.

Once the effect of dissipation for low velocity impact has been accounted for, we can return to the elastic model and assume the kinetic losses. This leads us to the following formula to model both elastic and low velocity impact losses.

$$\begin{cases} {}^{+}v = -\eta \cdot {}^{0}v = -\eta\, {}^{-}v \sqrt{1 - \left(\frac{v}{{}^{-}v}\right)^2}, & {}^{-}v \geq v \\ {}^{+}v = 0, & {}^{-}v < v \end{cases} \qquad \text{(EQ 41)}$$

1.6 Quantization effects

Accounting for low velocity impact has a remarkable effect on the observed results. Comparative simulations were conducted with and without the low velocity impact model. They led to the discovery of a quantization of the particle states. For a given non-dimensional acceleration, a particle initially dropped at random on the plate will experience a series of apparently random bounces until it lands softly on the plate. From that point on, the particle will be locked in a complex pattern of bounces that repeats periodically. Perturbation of the plate motion will either have no effect, or result in a transition to another quantized state. The transition will be operated through a series of bounces akin to a random walk. This is similar to a damping system[58].

1.6.1 Digital experiments

A series of experiments were conducted whereby a particle is dropped from a given height at time zero, with zero initial velocity. Computation of the successive impacts relies on

finding the first root of a rapidly oscillating function ((EQ 1) in Introduction). As stated in prior works cited in Section 1.3.2, classical numerical methods are notedly unreliable for the purpose of finding such roots. In order to have a reliable solution, we have developed an ad-hoc approach involving recursive symbolic Taylor expansion and root isolation in Mathematica™. This method will not be exposed here and is the topic of an upcoming publication [9].

The particle under consideration is assumed to be a point, so that rotational inertia is negligible. For the purpose of this model, air resistance is also neglected.

The resulting pattern of bounces was simulated under the classical and the low velocity impact models. Initial states are nearly identical, showing a motion akin to a random walk until the relative velocity of the particle with respect to the plate becomes small enough to trigger the low velocity impact model. The two model responses separate from that point on. In the case of the classical impact model, the particle appears engaged in a chaotic motion, while the low velocity impact results in a quantization of the states. Once the particle is captured by the plate, it will repeat a periodic, albeit complex, pattern of bounces.

1.6.2 Classical elastic impact model

A typical sample experiment conducted using this model was shown in Figure 1.10. The results concur with those of prior published research. In particular, one can observe the

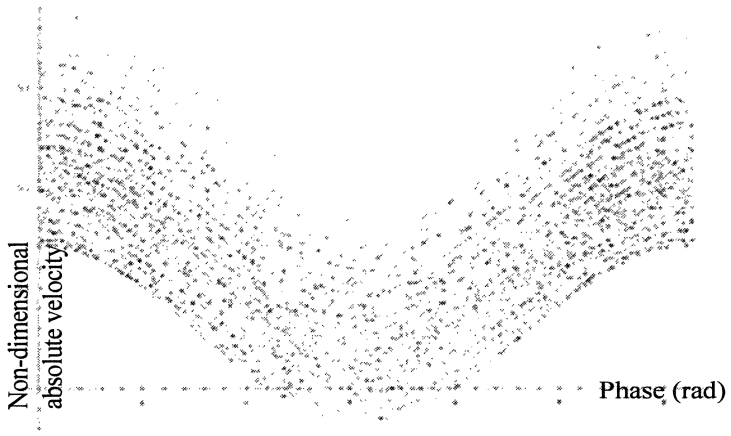

Fig:1.10 Poincaré diagram for the same conditions as in Holmes [3, Figure 7.d], same acceleration ratio of 10 (amplitude 2mm, frequency 35 Hz, coefficient of restitution 0.8) same number of representative points (5000).

typical horseshoe pattern identified by Holmes in 1982 [3], even though his model neglected the influence of plate height. The experiment conducted by Holmes [3, Figure 7.d] showing 5000 representative points was repeated and the result is shown here as Figure 1.10. Observe that even though the general horseshoe pattern is preserved, the point density found in our simulation is not as uniform as Holmes's. There appears to be a higher density towards the 2π ends of the phase. The lowest density is found near phase π. Physically, this corresponds to an accumulation of points near the plate peak position.

Likewise, Holmes identified the existence of strange attractors near the 2π phase. The same feature is exhibited in our results. It can be explain however by noticing that it corresponds to a series of small bounces occurring from the damping on the plate downswing and continuing on the upswing until the particle is ejected. This phenomenon was already encountered in Figure 1.5 and is repeated for an instance of Holmes' experimental condi-

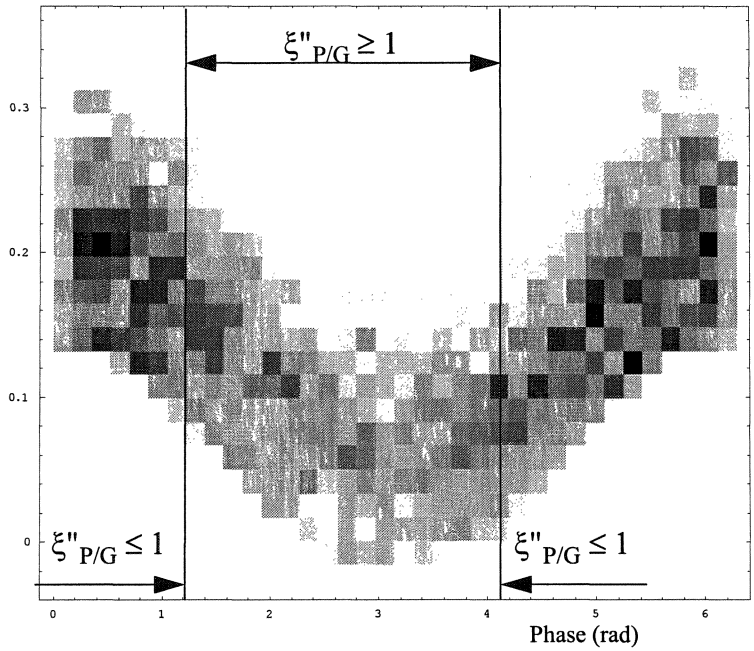

Figure 1.11 Density plot for the data in Figure 1.10 (white = zero density) showing the accumulation of points on the plate downswing and upswing.

tions in Figure 1.12. It is however an artifact of the model. As we shall see in Section 1.6.3, it disappears when quantization of impact velocity is taken into account.

1.6.3 Low velocity impact model

Using the same conditions as in Figure 1.2, but accounting for what happens at low relative velocity alters the results in a significant manner. Figure 1.13 shows the Poincaré diagram for conditions that are identical to Figure 1.2, modified to account for a minimum impact relative velocity of 0.4625 m/s. Observe that even though the number of computed bounces is the same as in Figure 1.2 (300), the number of representative points is significantly lower. Indeed most points are representative of an initial transition akin to a random

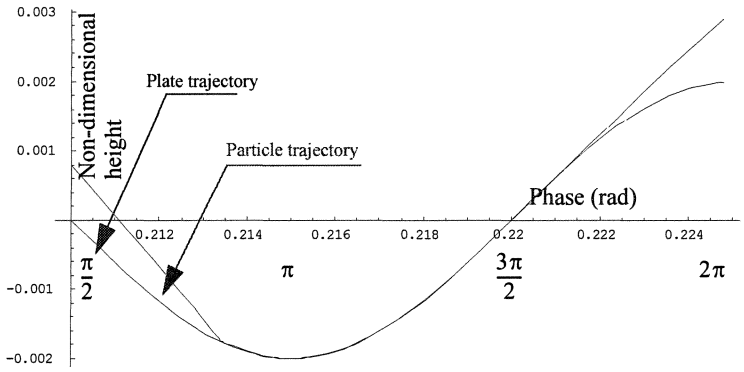

Figure 1.12 Illustration of the particle trajectory near a strange attractor in Holmes experiment [3].

walk. This transition period is nearly identical for figures 1.2 and 1.13. The two phenomena however part as soon as the relative impact velocity becomes small enough to be affected by the low velocity impact model. For Figure 1.12, The particle bounce is dampened when landing during the plate downswing. A series of small bounces (6 in this instance) ensues until the particle is ejected again from the plate surface. To clarify the relation to Figure 1.11 the phase angle (in radians) is shown below the time scale. For Figure 1.13, The non-dimensional critical impact relative velocity is 0.541 (corresponding to 0.46 m/s). After a series of apparently random bounces, represented by the collection of isolated points, the particle locks into a period-$_s$4 motion represented by the arrowed polygon. The corresponding pattern of bounces was shown in Figure 1.1. From that point on, the pattern of bounces in Figure 1.13 locks into a period-$_s$4 motion while the pattern in Figure 1.2 continues into chaotic motion.

A similar experiment was conducted for the conditions in Holme's [3] that were reproduced in Figure 1.10, but with a minimum impact velocity of 0.5 m/s. The resulting

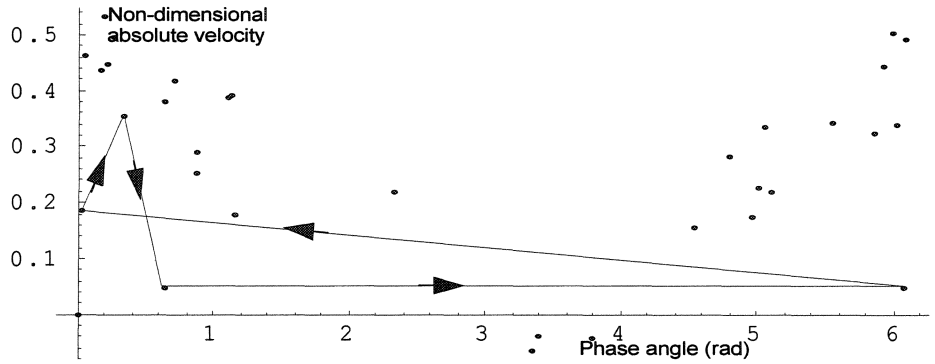

Figure 1.13 Poincaré diagram accounting for low velocity impact for the same conditions and number of points (300) as in Figure 1.2.

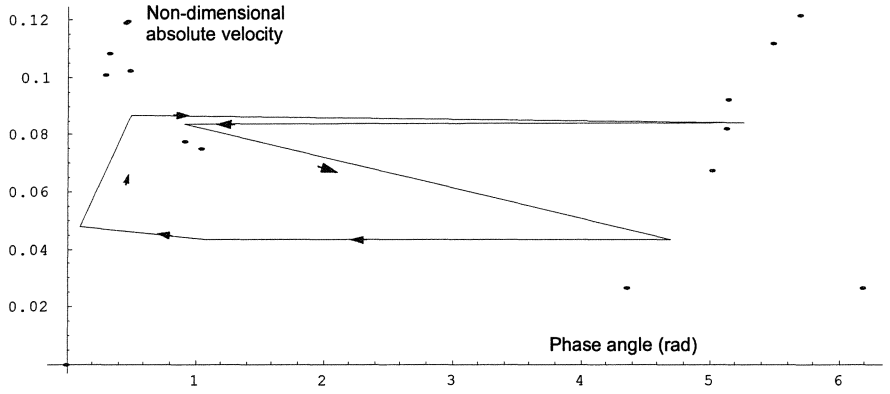

Figure 1.14 Poincaré diagram accounting for low velocity impact for the same conditions and number of points (5000) as in Figure 1.10. The trajectory corresponding to this diagram is shown in Figure 1.15.

Poincaré diagram is in Figure 1.14. It shows that after an initial series of random bounces, the particle motion locks into a period-$_s6$ pattern, the trajectory of which is shown in Figure 1.15.

1.6.4 Quantum influence

The main contribution of this work is the introduction of the low velocity impact model and its quantization effect on the motion, which is akin to "loss of ergodicity" of Hamiltonian system under non-hamiltonian perturbation[21]. If one omits to account for it, as was done in prior works, the motion generally appears to be chaotic. Hence, as one increases the number of simulated bounces, one also observes an increase in the number of representative points on the Poincaré diagram. As the minimum impact velocity is raised from zero, and the low velocity impact model is enabled, one observes that the motion will become periodic. Moreover the number of bounces in a period (i.e. number of cyclic points on the Poincaré diagram) will decrease as the minimum relative impact velocity increases. This effect is illustrated in the series of experiments shown in Figure 1.16, where the minimum impact velocity varies from 0 (a: classical model) to 0.2 m/s (b), 0.4 m/s (c), 0.6 m/s (d), 0.8 m/s (e). Note that the number of representative points decreases as

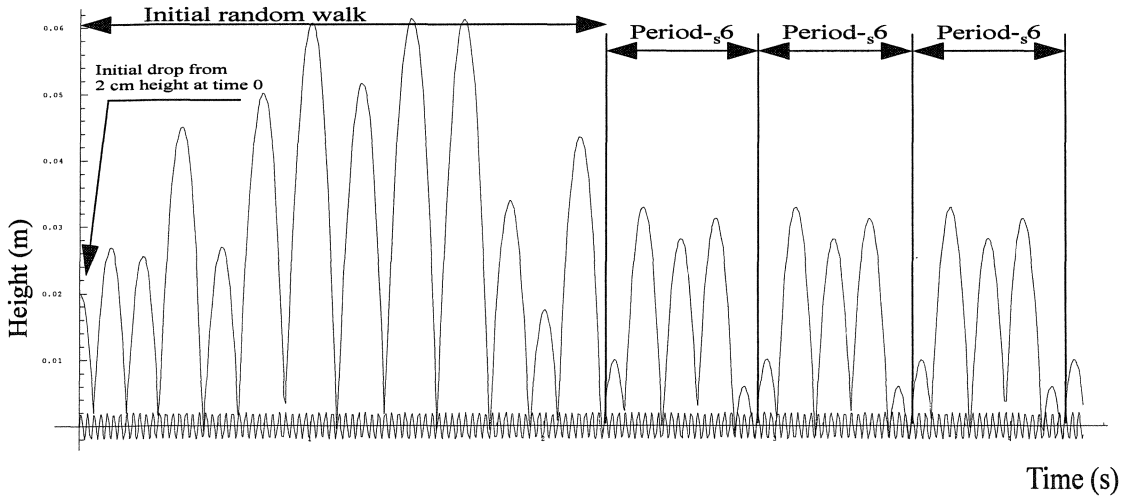

Figure 1.15 Particle trajectory for the Poincaré diagram of Figure 1.14. The trajectory shows an initial seemingly random bounces followed by periodic patterns.

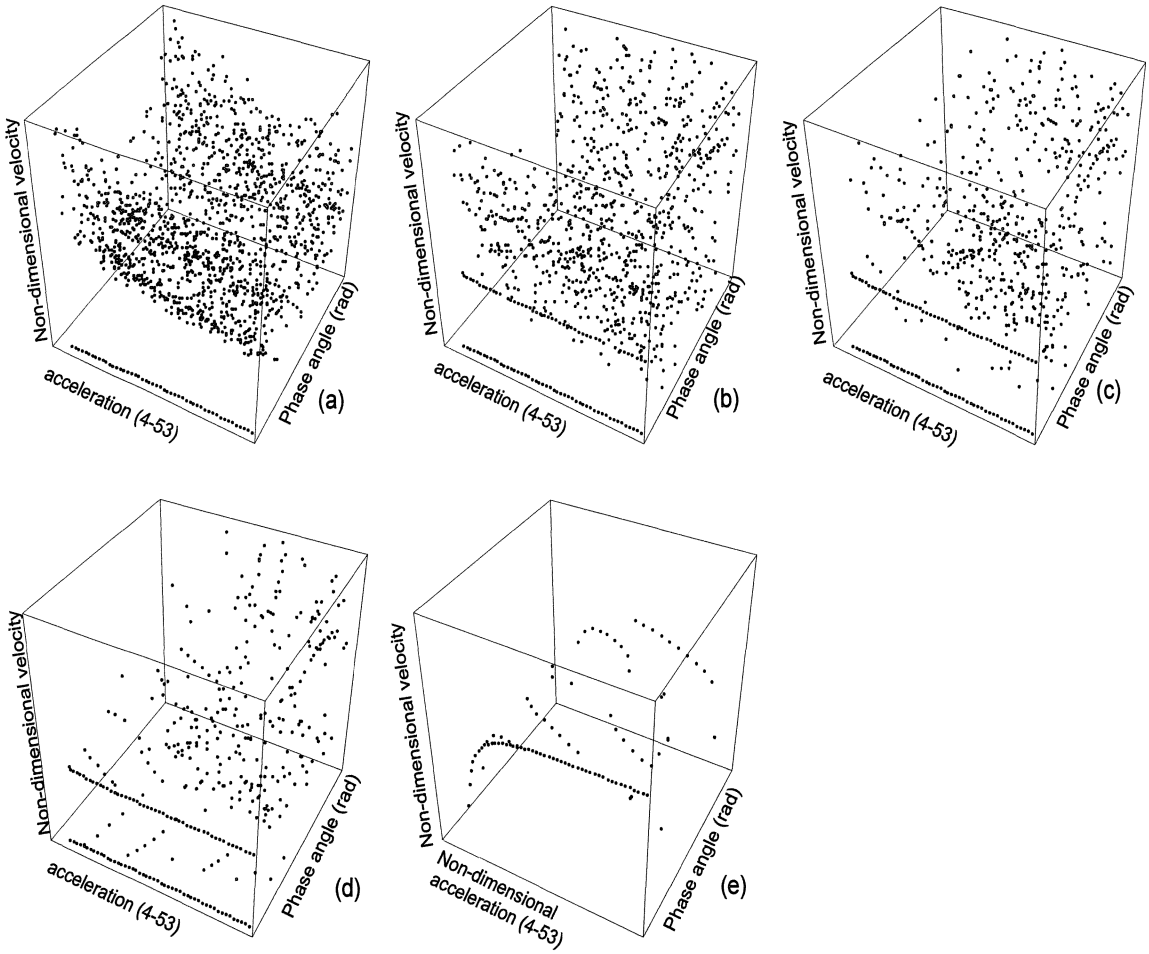

Fig:1.16 Each figure shows the collection of Poincaré diagrams representing the first 30 points for an acceleration ratio between 4 and 53.

the minimum impact velocity increases, denoting the occurrence of periodic bounce patterns over a decreasing number of points. The figures illustrate the Poincaré diagrams for a range of non-dimensional acceleration from 4 to 53. For each value of the non-dimensional acceleration, the first 30 bounces are computed. As the minimum relative impact velocity is increased, the number of representative points decreases, indicating the presence of a periodic motion.

1.6.5 Existence and unicity of quantized states

The question of existence and unicity of quantized states remains open to further research. One can observe, however, that the chaotic nature of the classical model dictates that each point on the Poincaré diagram will be visited exactly once, for else the motion would engage in a repeating pattern from that point onward. The Poincaré diagram for the classical model of elastic bounce thus produces a region covered by a cloud of points. Since no points can be repeated, the diagram becomes denser as the number of bounces increases as indicated by the graphs in figures 1.2 and 1.10. Assuming that the point distribution is stable as the number of sample increases, one can assume the existence of a probability density function over the Poincaré diagram and produce an experimental measure such as the one in Figure 1.11.

If one accounts for the low velocity impact model, the behavior of the particle will match that of the classical model almost exactly during the initial series of seemingly random bounces. That is, until the relative impact velocity happens to be small enough that the particle will remain on the plate. From that point on the particle will engage in a periodic motion. It is therefore legitimate to ask: **(1),** if such low velocity impact will indeed occur and **(2),** if such impact were to occur, would the repeating pattern be indeed unique.

On the first count, one can surmise, on experimental grounds illustrated by Figure 1.11 that a low velocity impact is bound to occur unless the random bounces diverge away from zero velocity. Indeed, the probability of a bounce occurring with less than critical

velocity is the integral of the probability density function (Figure 1.11) over a strip of height $\underset{\sim}{v}$. If the phenomenon is indeed chaotic, the probability of such an event will not be zero, hence the particle will eventually be captured by the plate.

While the above argument in the legitimacy of low velocity impact does not constitute a mathematical proof, it does however support the physics of the phenomenon. On that basis, we can answer on the second count, that of unicity. Once the particle is captured, the plate motion uniquely determines the boundary conditions for subsequent bounces. Since the mapping relating successive bounces is one to one [3], it means that the periodic mode is uniquely determined.

1.6.6 Stability of quantized states

Assuming that quantized states exist and are unique for a given plate motion (frequency & amplitude) the next question that arises is the stability of these states. Therefore, we studied those period-$_s$n motions to investigate the stability of those series of bounces, when subjected to a perturbation.

According to Floquet theory, the stability can be determined by computing eigenvalues of the matrix relating succesive periods. Every impact can be represented by the particle's velocity and position immediately following impact, for example, for a period-K motion, we can have:

$$\begin{pmatrix} v_{i+k} \\ h_{i+k} \end{pmatrix} = F\begin{pmatrix} v_i \\ h_i \end{pmatrix} = \begin{pmatrix} f_1(v_i, h_i) \\ f_2(v_i, h_i) \\ \cdots \\ f_k(v_i, h_i) \end{pmatrix} = \begin{pmatrix} F_1(v_i, h_i) \\ F_2(v_i, h_i) \end{pmatrix} \quad \text{(EQ 42)}$$

where: v_i and v_{i+k}, h_i and h_{i+1} are respectively the initial velocities and height after the i_{th} and $i+k_{th}$ impact.

$$\begin{pmatrix} \Delta v_{i+1} \\ \Delta h_{i+1} \end{pmatrix} = J \cdot \begin{pmatrix} \Delta v_i \\ \Delta h_i \end{pmatrix} \quad \text{(EQ 43)}$$

Letting Δv_i, Δh denote perturbations of initial conditions, one can evaluate the Jacobian of F. $J = \begin{pmatrix} j_{11} & j_{12} \\ j_{21} & j_{22} \end{pmatrix} = \begin{pmatrix} \frac{\partial F_1}{\partial v_i} & \frac{\partial F_1}{\partial h_i} \\ \frac{\partial F_2}{\partial v_i} & \frac{\partial F_2}{\partial h_i} \end{pmatrix}$ is Jacobian matrix. and is evaluated on the period-k orbit to study the growth rate of perturbations.

We will first consider the example of the period-4 motion exposed to a small perturbation

Figure 1.17:

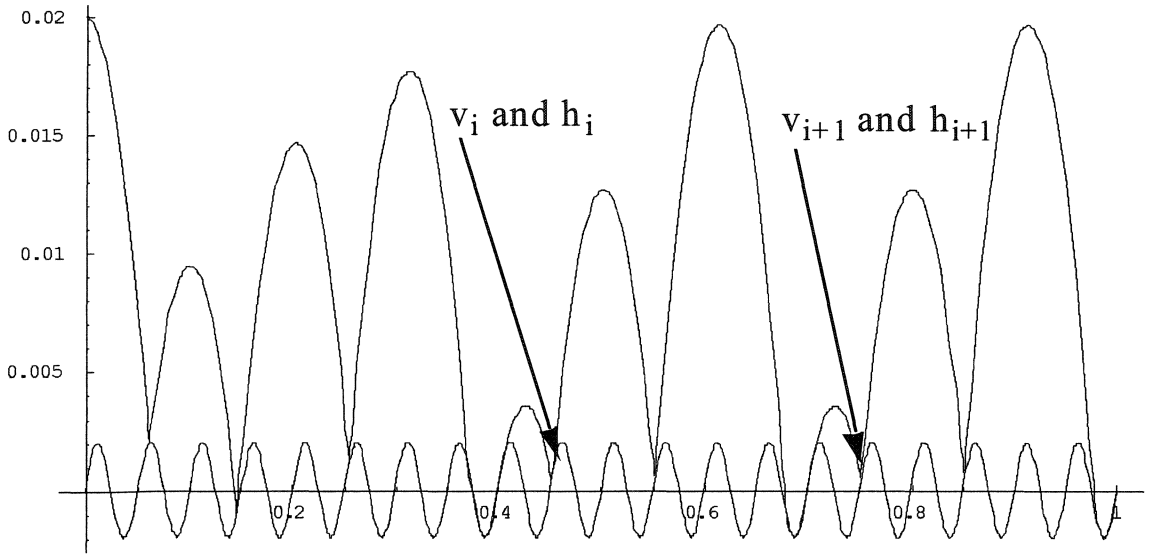

Fig:1.17 For the shown , h_i is: 0.0004665089419362 m, v_i is: 0.4891726722471415 m/s. h_{i+1} equals h_i and v_{i+1} equals v_i

$$\begin{cases} \begin{pmatrix} 0 \\ 0 \end{pmatrix} = \begin{pmatrix} j_{11} & j_{12} \\ j_{21} & j_{22} \end{pmatrix} \cdot \begin{pmatrix} 0.000001 \\ 0 \end{pmatrix} \\ \begin{pmatrix} 0 \\ 0 \end{pmatrix} = \begin{pmatrix} j_{11} & j_{12} \\ j_{21} & j_{22} \end{pmatrix} \cdot \begin{pmatrix} 0 \\ 0.000001 \end{pmatrix} \end{cases} \quad \text{(EQ 44)}$$

we can caculate the (EQ 44) for the Jacobian:

$$J = \begin{pmatrix} j_{11} & j_{12} \\ j_{21} & j_{22} \end{pmatrix} = \begin{pmatrix} 0 & 0 \\ 0 & 0 \end{pmatrix} \quad \text{(EQ 45)}$$

(EQ 45) (EQ 45) gives the eigenvalues of J: $\lambda \to 0$. which demonstrates that the system is locally stable.

When the perturbation is increased to a big enough value to change the periodical character, we have the following case:

$$\begin{cases} \begin{pmatrix} 0.10825 \\ -0.00115791 \end{pmatrix} = \begin{pmatrix} j_{11} & j_{12} \\ j_{21} & j_{22} \end{pmatrix} \cdot \begin{pmatrix} 0.024199 \\ 0 \end{pmatrix} \\ \begin{pmatrix} 0.11552 \\ -0.00104799 \end{pmatrix} = \begin{pmatrix} j_{11} & j_{12} \\ j_{21} & j_{22} \end{pmatrix} \cdot \begin{pmatrix} 0 \\ 0.002988 \end{pmatrix} \end{cases} \quad \text{(EQ 46)}$$

For clarification purposes we can express (EQ 46) as following:

$$\begin{cases} \begin{pmatrix} 4.47333 \\ -0.0478497 \end{pmatrix} = \begin{pmatrix} j_{11} & j_{12} \\ j_{21} & j_{22} \end{pmatrix} \cdot \begin{pmatrix} 1 \\ 0 \end{pmatrix} \\ \begin{pmatrix} 38.6612 \\ -0.350734 \end{pmatrix} = \begin{pmatrix} j_{11} & j_{12} \\ j_{21} & j_{22} \end{pmatrix} \cdot \begin{pmatrix} 0 \\ 1 \end{pmatrix} \end{cases} \quad \text{(EQ 47)}$$

$$J = \begin{pmatrix} 4.47333 & 38.6612 \\ -0.0478497 & -0.0350734 \end{pmatrix} \quad \text{(EQ 48)}$$

We can further derive the eigenvalues as $\lambda_1 = 4.25328$, $\lambda_2 = 0.0693144$. The eigenvalues clearly demonstrate that as soon as the perturbation is sufficiently large to break the periodical motion of the particle, it will change to chaotic bouncing. This change of motion will last until the relative velocity between particle and plate becomes smaller that the critical number. From that moment on, the particle will return to the previous $period-_s 4$ motion.

From an experimental standpoint, one must acknowledge that detecting periodic modes becomes extremely difficult in practice. As the stability of the phenomenon decreases, the motion will appear more and more chaotic when being perturbed. Moreover, experimental observations become less likely as the slightest perturbation will induce a chaotic response.

1.7 Conclusion

The question of the vibrational response of shallow powder bed arises in the context of powder mechanics. Typical theoretical analysis is conducted on the basis of the response of a single particle bouncing off a sinusoidally excited plate. The research presented here derives from an attempt to model experimentally observed, yet heretofore unexplained powder behavior in a novel dry powder nozzle. While experimental research is still ongoing, the model developed here is original.

The main contribution of this paper hinges on a heretofore undetected vibrational mode in which a particle bouncing off a vibrating plate lands with low relative velocity and is captured by the plate. In order to better model low velocity impact, a new model of elastic bounce is introduced whereby the particle is forced to exchange a minimum "quantum" of kinetic energy with the plate.

The main consequence of this model is that, contrary to most published results to date, the particle behavior is not chaotic. In fact, every plate vibration mode is associated with an "allowed" state. A particle bouncing off such plate will experience an apparently random series of bounces until it becomes "trapped" in this allowed state. A perturbation of the motion will either have no effect, or result in a random walk transition toward another allowed state.

CHAPTER 2

VIBRATIONALLY INDUCED FLOW IN A MICRO L-VALVE

2.1 Abstract

With the exception of manual sand-painting, dry powder flows at very low mass flowrates have never been achieved in industrial settings. A novel vibrationally actuated micro L-Valve was shown to produce scalable flowrates within a fraction of a milligram per second with rough uncalibrated WC powders. This article is concerned with the experimental flow characterization in a micro L-Valve. In general, three flow modes were identified when scanning in frequency at constant amplitude. In the first mode, no flow occurs until a trigger frequency is reached. The flowrate then ramps up, peaks and ramps down until it eventually stabilizes and remains constant in the last and third mode. The third mode was further investigated to test the stability of the flowrate. Experiments indicate that flowrates remain independant of frequency in the third mode and are repeatable. The powder load in the shaker appears to have no noticeable influence until a final emptying phase is reached.

The main contribution of this paper is an experimental characterization of vibrationally induced dry powder flows in a novel micro L-valve. The ultimate objective of this research is to enable control of both powder flowrate and powder deposition. The scope of this paper is limited to flow characterization.

Industrial powder flow control is typically operated at large gas-fluidized flowrates (order of liters/second) [25]. Low flowrates of gas transported powders were recently introduced in laser consolidation and powder processing [29]. However, flow control and deposition remains a challenge. To our knowledge, the novel micro L-Valve introduced here is the first dry powder low mass flow control apparatus.

The body of literature concerning micro flow control of powders is nearly empty. To our knowledge, dry powder transport at the flowrates addressed herein has never been done. Theoretical studies of such powder flows are also nearly abscent from prior works, with the exception of the author's contributions[9][44].

After a short summary of the few applicable prior contributions, this article will introduce experimental set up and results. A summary description of a proprietary nozzle and its actuation, instrumentation and control will be presented. The recorded experimental flow-rates will be presented for a range of frequency / amplitude effectively affecting mass flow control. Materials experimented with include spherical glass and stainless steel 316

with respective diameters $22\mu m$ and $\sim 10\mu m$, and coarse SiC, cement, and WC. Only the experiments conducted with WC powder will be reported here.

2.2 Prior works

The L-Valve is a specific type of a generic class called a "non-mechanical valves" [22][26]. It typically consists of a downcomer section and an elbow with an aeration point inserted at their junction [25][26].

The major parameters affecting solids flow in L-shaped valves and their characteristics were first described almost three decades ago, aiming to improve the understanding of handling and storage of granular materials in industrial applications [22][26].

The problem at hand finds its origin in new manufacturing technologies that either necessitate or would greatly benefit from low dry powder flowrates and deposition. Low flowrates application include powder material processing, and pharmaceutical metering. Examples of free form fabrication technologies that would greatly benefit from low flowrates and deposition are selective laser sintering (SLS), laser engineered net-shaping (LENS), 3D Printing and laser consolidation [25]. The problems associated with the characterization of small powder flows (ranges below 1000 mm^3s^{-1}) were addressed several years ago [29]. However despite the efforts made, both flow and deposition of powders

were highly irregular and the problems of small flows and location of a powder deposit remained unsolved for the existing dry powder transport systems [4].

2.3 Experimentals

Early implementation of this research relies upon Taguchi's design of experiment approach [22][41]. After identifying the process parameters, objective and internal variables, an experimental apparatus was implemented to extract an empirical relation.

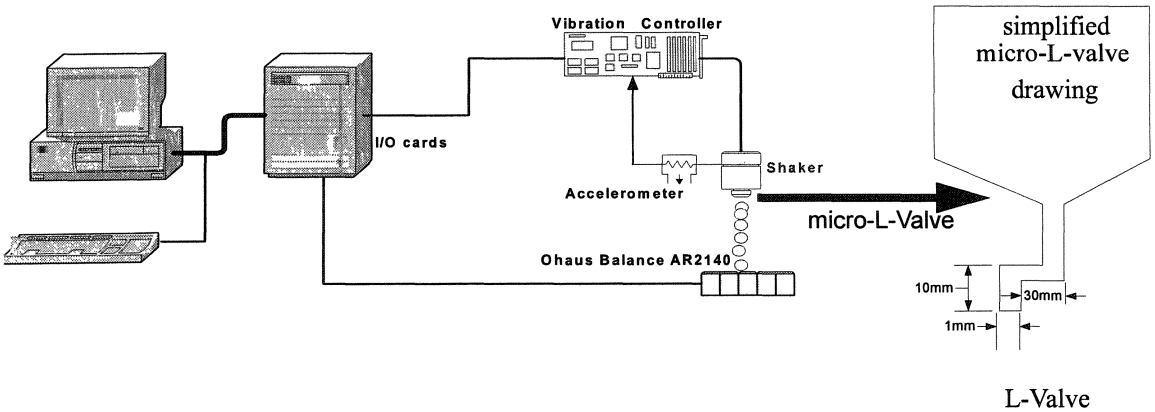

Figure 2.1: Basic experimental setup used for the experiment.

2.3.1 Process parameters

The process parameters identified using Taguchi's design of experiments [22] are presented in Table 1.

Table 1: Design of experiment parameters

Process Parameters	• Amplitude • Frequency • Material • Nozzle material and geometry.
Objective Criteria	• Mass flowrate
Internal Variables	• Remaining mass in nozzle

2.3.2 Experimental set up

The basic experimental set up is shown in Figure 2.1. A micro L-valve was mounted to a VTS shaker (vibration test system model number: DVC-4 sine), and subjected to a vertical vibration at frequencies below 100 Hz. The acceleration of the shaker was measured by an accelerometer (ICP 353B18).

Even though more than ten valves were tested, only three will be presented in this paper. The shape of the interior part of the valves was the same for all the samples, designed as a channel with bisections as squares, however the height (d) ranged from *1mm* to *3 mm.*

The powders used were coarse tungsten carbides (**WC**). The physico-chemical properties of this material are given elsewhere [29]. The real time deposition velocity was measured by an instrumented high resolution scale using *LabView*^{TM}.

2.3.3 Overview of the experiments

The primary experiment was conducted to characterize the mass flowrate as a function of frequency at a given amplitude. Experiments revealed the existence of three modes. The first one occurred at frequencies below 40Hz, which is below the limit at which flow could exist (Figure 2.2). As the frequency increases, the flowrate entered a second mode in which it increased, peaked and decreased. Finally, in the third mode, the flowrate reached a constant value independent of the frequency Figure 2.2.

The remaining sections will focus on the third mode as it presents the advantage of a constant flowrate. In Section 2.3.6 we shall investigate the influence of the powder load in the nozzle. Finally, in Section 2.3.7 we shall question the stability of the flowrate as a function of frequency. The last section will discuss the result achieved to date.

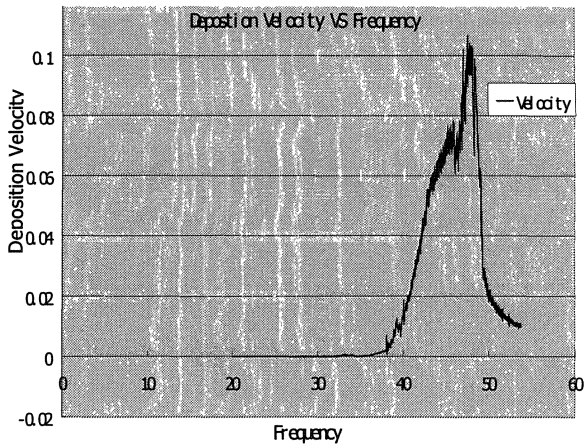

Figure 2.2 The variation in deposition velocity at low frequencies (ranging from 20Hz to 53H)

2.3.4 Mass flowrate vs lower frequency

The powder mass flow rate at lower frequency is presented in Figure 2.2

The height of the valve *d* was given by the type of the valve (1 mm), and the vibration amplitude was locked to 0.015 in so that frequency was the only parameter that varied and had effect on the powder flowrate.

The measurements revealed a reproducible pattern whereby the flow is non existent until a frequency of 35 Hz is reached. The flow rate then steadily increases until it peaks at 46Hz. From there, the flowrate then drops down rapidly to stablize at about 50 Hz. We can clearly distinguish three flow regimes. One corresponding to a low energy domain where powder essentially bounce on the lower plate alone, a transition regime where powders

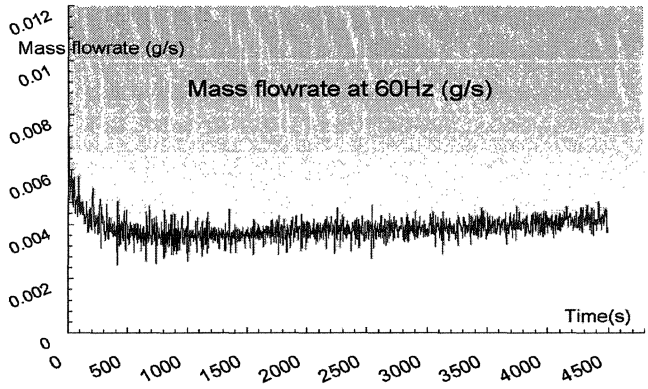

Figure 2.3 Mass flowrate vs time at 60 Hz.

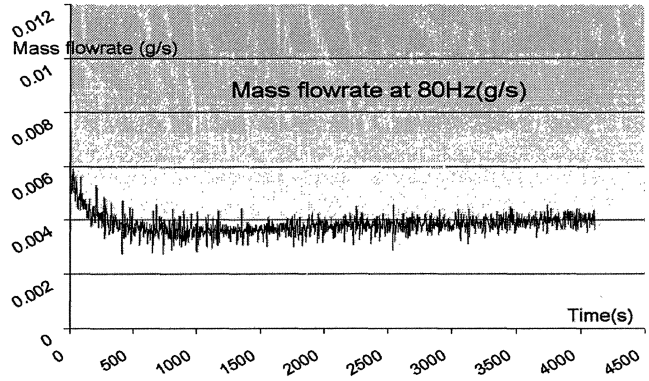

Figure 2.4 Mass flowrate vs time at 80 Hz.

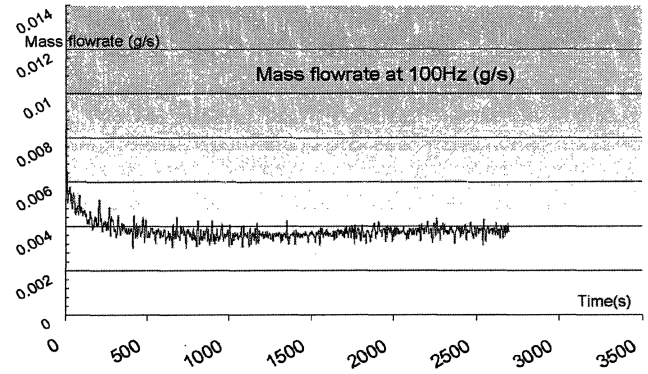

Figure 2.5 Flowrate vs time at 100 Hz.

bounce between the two plates but in no repeatable pattern, and finally a periodic mode of vibation at the plates frequency. These pattern are reminiscent of those observed in the two plates problem [44]. .

2.3.5 Flow stability at high frequency

Experiments conducted at higher vibration frequencies (60, 80, 100 Hz) showed that when the vibration amplitude and the plates interstitial distance *d* were kept constant the deposition flowrate was independant of frequency. As illustrated in figures 2.3,2.4, and 2.5, the flowrate was stable at about 4mg/s.

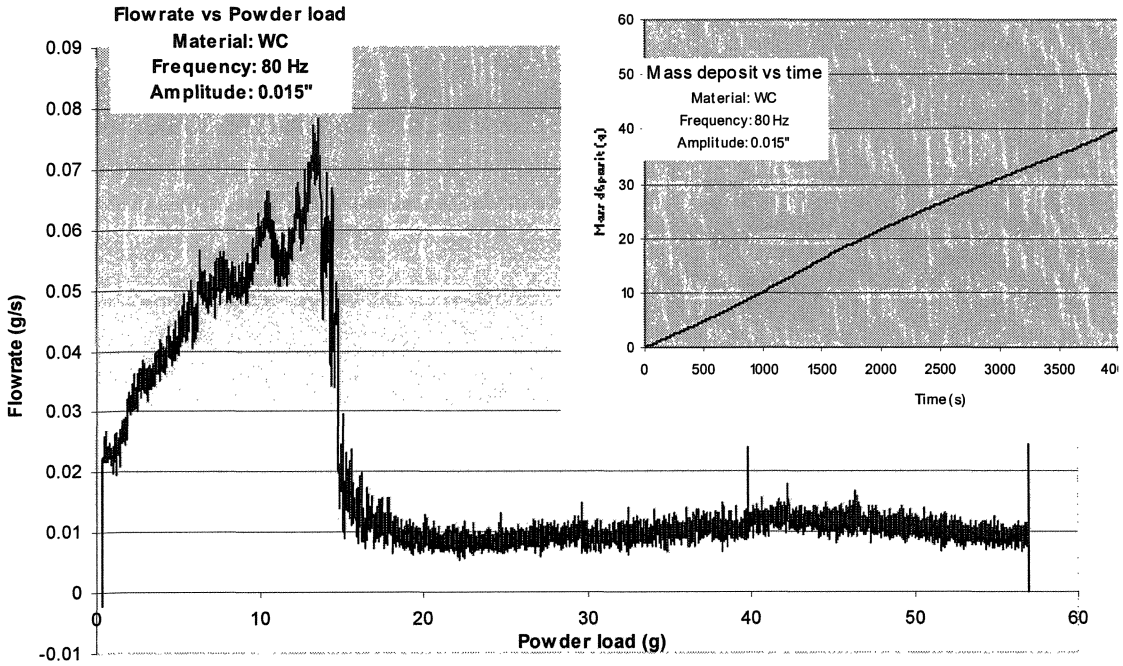

Figure 2.6 58 grams initial load, evolution of flowrate vs powder load showing a final "emptying mode" below 15 grams.

2.3.6 Flowrate vs powder load

The results from our experiments also demonstrated that the powder flow deposition rate was also affected by the powder load (the mass of powders inside the valve reservoir). As shown in Figure 2.6, 58 grams of WC powder were initially loaded into the L-valve reservoir. The reservoir was then emptied at 80Hz. The mass flowrate was constant at about 10mg/s until the remaining mass reached down to about 16 grams. This fluctuation continued until the valve was completely emptied. This emptying behavior was shown to be repeatable however.

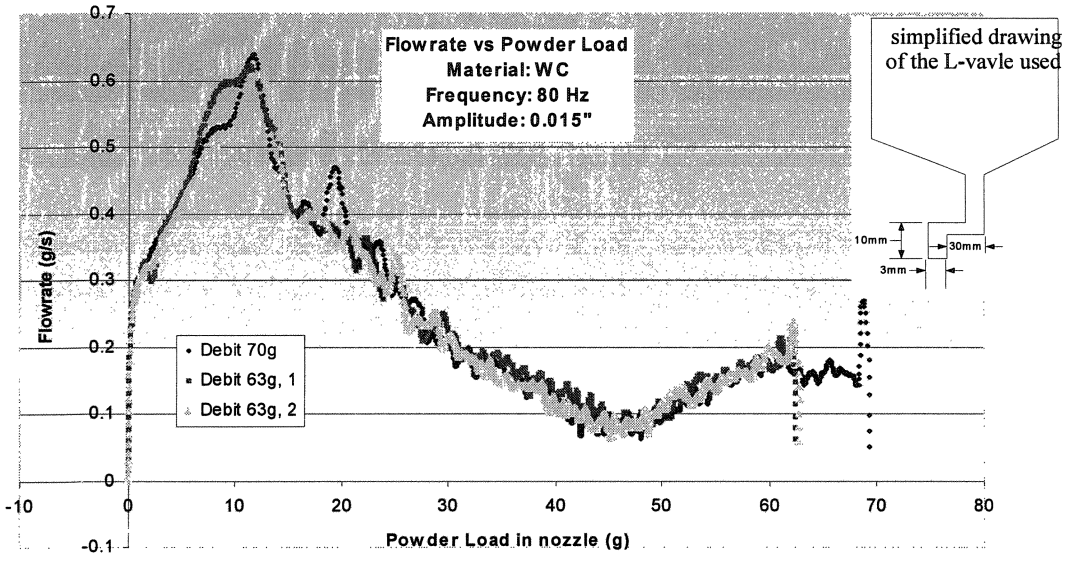

Figure 2.7 Mass flowrate vs powder load for 3 different experiments.

2.3.7 Repeatability of flowrate

In order to test the hypothesis that the remaining mass in the reservoir was indeed an internal variable to the process, a series of experiments were conducted where flowrate was measured as a function of remaining mass. Three experiments were carried out with powder load being the only variable (other conditions were maintained constant). The corresponding measurements are shown in Figure 2.7. For the same valve structure (inner height of 3 mm), the results revealed an astonishing repeatability of the phenomena, with flow rates almost overlaping each other. That the flowrate was different from Figure 2.6 is attributed to the differences in valve geometry as the hight of the valve used in the previ-

ous experiment was thinner (1 mm). The effect of the geometry dimension on the powder flowrate is clearly demonstrated here and it was disscussed in detail in our theoretical study [44].

2.3.8 Discussion

The results from our experiments are critical for a good understanding and control of powder flows in a vibratory L-Valve.

One of the most valuable results of this experimental work is to show that valve geometry, materials, and vibration amplitude and frequency completely determine the mass flowrate through a micro L-Valve. This is an important result if one is to assert control over powder flows. The flowrate response curve to frequency is also an important determinant of flow control and we have shown its repeatability. Indeed, an important result is the confirmation that flowrate becomes constant over a certain frequency.

The experiments conducted with other powders (glass beads, stainless steel and Portland cement) exhibited the same pattern of behavior at high frequency, regardless of powder type and shape. In all three cases, the flowrate started to fluctuate when the powder load entered an emptying mode. In addition, the repeatability of the experiments verified that for the same type of L-valve, the flowrate at a given frequency is not only predictable, but that the flowrate can be controlled by using different types of valves. It remains that the

exact frequency at which different powders will start to fluctuate will depend on the type of the powder. Therefore we can assert that the type of material used will affect the flow-rate, however as presented in Figure 2.7, apart from the peak position, there was no significant difference in the flowpattern of the three materials tested (glass beads, stainless steel and WC).

The differences in the powder flowrates observed in Figure 2.3- 2.5, Figure 2.6 and Figure 2.7 occured due to the differences in the types of valves employed in those experiments. The valve presented in simplified drawing in Figure 2.1 used in experiments 1-5 (Figure 2.1-2.5), had an interior hight *d* of 1 mm, the valve depicted in Figure 2.7 had a 3 mm height. The valve used in Figure 2.6 had a height of 2 mm.

The effect of channel height on powder flowrate does play an important role which still needs to be further studied.

During different runs of the experiments, it was observed (these data are not presented) that when shaken at constant amplitude (at 200 Hz) both valves produced constant flow-rates. When the frequency was lowered to about 90 Hz, the smaller valve (1 mm) remained constant, while the larger one (3 mm) began to fluctuate. When we decreased frequency to 60 Hz, even the flowrate from the smaller valve started to fluctuate, as presented in Figure 2.2.

These results indicate that at higher frequencies the flowrate will be constant regardless of the type of L-valve employed. However, at the lower frequencies, the valves with smaller channel height will reach the constant flowrate faster, while the ones with the larger channel height will require higher frequencies. A theoretical explanation of this phenomena can be drawn from the study of the two plates problem [44].

2.4 Conclusion

The experimental work reported here pertains to the flowrate characterization of a novel type of metering device for dry powders at very low flowrates. To our knowledge, no prior device of this type has ever existed, let alone be observed. The apparatus consists of a nozzle with a horizontal neck vibrationnally actuated along the vertical direction. Experiments designed to establish if there was a relationship between vibrations and flow have demonstrated that the vibrational response is repeatable. Process parameters were identified as vibrations amplitude and frequency, density of the particle materials, and geometry of the nozzle. The only internal variable is the remaining mass in the reservoir, though its influence is limited to the emptying mode and may just be an artifact of the convection cells. The flow rates appears to follow a pattern whereby flow occurs and increases linearly from a trigger frequency. The flowrate peaks, then decreases linearly until it reaches a constant value at higher frequencies. Although further experimental work is still needed, the results to date concur qualitatively with our theoretical analysis.

CONCLUSION

Anticipated impact

From a scientific standpoint, the research presented here advances the state of knowledge concerning vibrationally fluidized granular material flow. From a technological standpoint, it was motivated by a recognized opportunity to advance the state of the art, and indeed contributes, a potential quantum advance in powder based free form fabrication.

The anticipated impact of this work, however, is much broader than its initial scope. Already, applications are emerging in areas dealing with dry powder flowrate control, such as powder plasma, vacuum or controlled atmosphere processing. Pharmaceutical applications also loom heavy on the horizon of potential applications (e.g. precise dosage of custom pills.) In the FFF domain, the addition of powder flow control and deposition opens possibilities heretofore unavailable. For example, we envision that one will be able to alter the build material at will during fabrication and design such complex fonctions as material gradient and porosity into a structure. The primary target for such application are biomedical implants.

Specific contributions

The present thesis contributes to both modeling and analysis aspects of granular material mechanics, and provides hints of experimental validation. Specifically, these contributions focus on the response of shallow powder beds to vertical vibrations of either a support plate or an enclosing channel. An ancillary contribution came for the need for a robust root finding algorithm to a combination of rapidly varying transcendental and polynomial functions. To our knowledge, the study of the vibrational response of a shallow powder bed in a micro channel is a first. So is its experimental counterpart consisting of flow measurements.

a Modeling and analysis

Computational tool development: Prior investigations into the modeling and simulation of a particle bouncing off a vibrating plate were burdened with the difficulty of numerically finding the moment of impact. That time is determined as the first root of a rapidly oscilating function containing quadratic and sine terms. Prior works did acknowledge both the difficulty and the dependence of the conclusion on a robust solution. To our knowledge, the root finding strategy we developped is new. It uses a combination of numerical and symbolic computations. It proceeds first from a root isolation method based on bounds on the functions, then once the first suitable region is found, a recursive Taylor expansion is used on this region or a subdivision thereof. Symbolic root isolation

methods available in Mathematica™ are used on the Taylor expansion until a suitable domain is found for numerical methods to apply relyably.

Single plate problem: The single plate problem is defined as one particle bouncing off a horizontal vibrating plate. Although this problem is only partly relevant to the micro channel (two plates) problem, it provided an excellent test bed to buid expertise towards our aim. Furthermore, this problem does have some degree of relevance to the feed reservoir of the nozzle since it is akin to a vertically vibrated open container. Yet, in the process of replicating and evaluating prior works, a number of significant advances were made.

1. Although periodic bounce responses had been identified before, a new type of sub-harmonic response was identified, which we called period-$_s n$. In such a motion, the particle experiences a repeating pattern of complex pattern consisting of bounces, at the end of which the particle lands on the plate without bouncing until it is thrown off again and repeats the bounces.

2. The discovery of period-$_s n$ motions, led to the remark that elastic impact models are inadequate to represent low velocity collisions. A new *soft landing model* was introduced that accounts for a minimum "quantum" of kinetic energy to be exchanged with the plate. Interestingly, this model leads to velocity transformation equations similar to that of relativist kinematics. Just like their relativist counterpart match classical mechanics to a high degree of accuracy until nearly the limit velocity (speed of light),

our new model matches classical elastic collision until a minimal impact velocity is nearly reached.

3. The tiny chink introduced in the laws of elastic collision by the soft landing model has profound ramifications on the problem at hand. Just as in quantum mechanics the quantization of energy exchanges forces particles into quantized states, so does the soft landing model. Our research shows that for a given amplitude, frequency, coefficient of restitition and minimal impact velocity, only one stable response can exist on the plate. The soft landing model dictates that after an apparently random series of bounces, the particle will eventually lock into a complex periodic pattern of bounces. We can speculate that this striking observation may be representative of a general class of quantized response to vibrational excitation. In the one-plate problem nevertheless, this remark leads to a significant departure from prior works.

b Experimental

The experimental flow characterization experiments conducted in this research also constitute a first. Their most important results to date was to show the repeatability of the observed flowrates as a function of process parameters. This constitutes therefore an experimental confirmation that flowrate control is indeed feasible. The observed flowrates support the one particle approximation adopted in the two plates problem. The transition states in the flowrate are in qualitative agreement with the two plates model.

c Intellectual property

The research reported here carries the elements of feasibility and demonstration needed to support intellectual property claims on the micro vibratory L-valve. In particular, the analytical part of this research provides an insight into the mechanics of the micro-channel, while the experimental part demonstrate the feasibility of flow control.

Recommendations for further research

As this research currently stands, the one plate problem would benefit from further minor refinements. The question of quantization would explain some of the observed powder bed expansions when scanning in frequency. However, this will remain a conjecture until experimentally demonstrated. Should this experimental demonstration be achieved, the theoretical questions concerning existence and unicity of the steady state periodic solutions are still open.

The two plate problem is also in need of further theoretical investigations. Now that the periodic responses have been identified by means of digital experiments, further mathematical analysis indicating existence and transitions of these modes is needed. This model would in turn be useful in the design of nozzles.

In order to apply the MVLV to its initial intended purpose, one should also be concerned about powder projection and deposition. The modeling of powder droplets impacting the substrate, as well as its resulting geometry is an open problem. Its experimental applications relates directly to the feature definition in sand painting.

The objective of further research will therefore to further develop understanding of the powder flow control and of the powder deposition processes in order to apply them to the drawing of powder patterns in layers. The completion of this research is a critical milestone on the way to a powder based free form fabrication process capable of altering the local build material as well as its properties.

REFERENCES

[1] KIPOM, K., PAK, H.K. AND CHANG, I.(1999). Velocity Profiles of Subharmonic Waves in Granular Materials, Journal of the Korean Physical Society, 34 (6), 538-541.

[2] JAEGER, H.M.AND NAGEL, S.R. (1992). Physics of the granular state, Science **255** (5051) 1523-1531.

[3] HOLMES, P.J. (1982). The dynamics of repeated impacts with a sinusoidally vibrating table, Journal of Sound Vibration, 84(**2**), 173-189.

[4] WOOD, L.A.AND BYRNE, K.P. (1981). Analysis of a random repeated impact process, Journal Of Sound and Vibration **78**, 329-345.

[5] HJELMFELT JR, ALLEN T. (1989). Chaotic behavior of particle on vibrating plate, J. Eng. Mech., 115(**7**) 1458-1471.

[6] LUO, A.C.J. AND HAN, R.P.S.(1996). Dynamics of a bouncing ball with a sinusoidally vibrating table revisited, Nonlinear Dyn 10(**1**) 1-18.

[7] BRENNEN, C.E. (1996). Vertical Oscillation of a Bed of Granular Material, J. Applied Mechanics, 63(**1**) 156-161.

[8] SONDERGAARD, R., CHANEY, K., BRENNEN, C.E. (1990). Measurements of solid spheres bouncing off flat plates, J Appl Mech 57(3) 694-699.

[9] ZHU, J. AND PEGNA, J.(2003). Recursive Taylor expansion and root isolation... chaotic root finding, manuscript.

[10]JENNINGS, M.J., TO, DONG VU, WILLIAMS, K.A. (2000). Dynamics of an elastic ball bouncing on an oscillating plane and the oscillaton, Appl Math Model 24(10) 715-732.

[11] FARADAY, M.(1830), Philos. Trans. R.Soc.London 52, 299.

[12] JAEGER, H.M., NAGEL, S.R. AND BEHRINGER, R.P.(1996). Granular solids, liquids and gases, Rev. Mod. Phys. **68** (4) 1259-1271.

[13] GEMINARD, J.C. AND LAROCHE, C.(2002). Energy of a single bead bouncing on a vibrating plate: experiemnts vs numerical simulations, Physical Review E. http:// www.ens-lyon.fr/~geminard/bead.pdf

[14]PEGNA, J. (1995). Application of Cementitious Bulk Materials to Site Processed Solid Freeform Construction, Proceedings of the Solid Freeform Fabrication Symposium, Ed. by H.L Marcus, J.J. Beaman, D.L. Bourell, Joel W. Barlow, and R. H. Crawford,

Austin, Tx, pp.39-45.

[15] EGGERS, J. AND RIECKE, H.(1999). A continuum description of vibrated sand, Phys. Rev. E. **59** (4), 4476-4483.

[16]GUTMAN, R.G. (1976). Vibrated beds of powders Part I: A theoretical model for the vibrated bed, Trans. Instn. Chem. Engrs. **54**, pp. 251-257.

[17]] MELO, F., UMBANHOWAR, P. AND SWINNEY, H. L. (1995) Phys. Rev. Lett. **75**, 3838.

[18] UMBANHOWAR, P. , MELO, F. AND SWINNEY, H. L. (1996) Nature **382**, 793.

[19] E. CLEMENT, L. VANEL, J. RAJCHENBACH AND J. DURAN. (1996), Phys. Rev. **E53**, 2972.

[20] T. H. METCALF, J. B. KNIGHT AND H. M. JAEGER (1997), PhysicaA236, 202.

[21]A.J.LICHTENBERG, M.A.LIEBERMAN. (1992). Regular and Chaotic Dynamics. Springer-Verlag, New York.

[22]TAGUCHI, G. (1993). Taguchi on Robust Technology Development. ASME Press,

NY.

[23]PEGNA, J., BERGÉ, R., PATTOFATTO, S., QUINSAT, Y., AND TERRIER, M.(2000); "Experimental Characterisation of Powder Flow and Deposition of a Vibratory L-Valve," Proceedings of the Joint IDMME-CSME Forum 2000, Ed. by C. Fortin, C. Mascle and J. Pegna, Montreal, Quebec.

[24]PEGNA, J.(1997). Exploratory Investigation of Solid Freeform Construction, Automation in Construction, Vol. 5, no.5, pp. 427-437

[25]WOODCOCK, C.R. AND MASON, J.S.(1987). Bulk Solids Handling, Leohard Hill.

[26]PEGNA, J.(1995). Application of Cementitious Bulk Materials to Site Processed Solid Freeform Construction, Proceedings of the Solid Freeform Fabrication Symposium, Ed. by H.L Marcus, J.J. Beaman, D.L. Bourell, Joel W. Barlow, and R. H. Crawford, Austin, Tx, pp.39-45.

[27]PEGNA, J.(1995). Exploratory Investigation Of Layered Fabrication Applied To Construction Automation, Proceedings of the ASME Design Technical Conferences, Design Automation Conference, Sept. 17-21, Ma., DE-Vol. 82, pp.219-226.

[28]MARCUS, R.D. ET AL(1990). Pneumatic Conveying of Solids, Chapman and Hall.

[29]SCHWENDNER, K.I., BANERJEE, R., COLLINS, P.C., BRICE, C.A., FRASER, H.L. (2001). Direct laser deposition of alloys from elemental powder blends. Scripta Materialia 45: 1123-1129.

[30]WOOD, L.A.AND BYRNE, K.P.(1981). Analysis of a random repeated impact process, Journal Of Sound and Vibration **78**, 329-345.

[31]HOLMES, P.J.(1982). The dynamics of repeated impacts with a sinusoidally vibrating table, Journal of Sound Vibration, 84(**2**), 173-189.

[32]HJELMFELT JR, ALLEN T.(1989). Chaotic behavior of particle on vibrating plate, J. Eng. Mech., 115(**7**) 1458-1471.

[33]LUO, A.C.J. AND HAN, R.P.S.(1996). Dynamics of a bouncing ball with a sinusoidally vibrating table revisited, Nonlinear Dyn 10(1) 1-18.

[34]BRENNEN, C.E.(1996). Vertical Oscillation of a Bed of Granular Material, J. Applied Mechanics, 63(1) 156-161.

[35]PEGNA, J. AND ZHU, J.(2003). Quantization effects in shallow powder bed vibrations, Eliza M. Haseganu memorial volume on "Advances in Continuum Mechanics," Arde Guran, Andrei Smirnov and David Steigmann Eds., Stability, Vibration

and Control of Systems, World Scientific Publ.

[36]ROCK AND GILMAN(1995). A New SFF Process for Functional Part Rapid Prototyping and Manufacturing: Freeform Powder Molding, Proceedings of the Solid Freeform Fabrication Symposium, Ed. by H.L Marcus, J.J. Beaman, D.L. Bourell, Joel W. Barlow, and R. H. Crawford, Austin, Tx, pp.80-87.

[37]SACHS, E., CIMA, M., CORNIE, J.(1990). Three Dimensional Printing: Rapid Tooling and Prototypes Directly for a CAD Model, Annals of CIRP, Vol.39, 1, pp. 201-204.

[38]DECKARD AND BEAMAN (1987). Solid Freeform Fabrication and Selective Laser Sintering, Proceedings of the 15th NAMRC-SME.

[39]BROWN AND RICHARDS (1982). Principles of Powder Mechanics, Pergamon Press, 2nd ed.

[40]HANS (1990). "Particle Technology", Chapman And Hall, N.Y.

[41]TAGUCHI (1987). System of Experimental Design I & II, UNIPUB Kraus International Publications.

[42]WOODCOCK, C.R AND MASON, J.S. (1987). Bulk Solids Handling. Bell & Bain Ltd,UK.

[43]KNOWLTON, T.M. AND HIRSAN, I. (1978). L-valves characterizied for solids flow. Hydrocarbon Processing **57**: 149-156.

[44]J.ZHU AND J.PEGNA. Shallow beds between sinusoidally occilsting plates, under preparation.

[45]J. ZHU ET AL (2003). Powder Deposition and Experimental Flow Characterization of a Vibratory L-Valve, ASME, Chicago

[46]MASATO SAEKI, TOSHINORI MINAGAWA AND EISUKE TAKANO (1995). Study on Vibratory Conceyance of Granular Materials, Trans.Jpn.Soc.Mech.Eng., Vol.63, No.615.C[46]

[47]A.DRESCHER (1992). On the criteria for mass flow in hoppers, Powder Technology, 251-260.

[48]C.E.DAVIES AND J.FOYE (1990). Flow of Granular Material Through Vertical Slots, CHEMECA Symposium, Auckland, New Zealand.

[49]ZHU, J. AND PEGNA, J. (2003). Recursive Taylor expansion and root isolation... chaotic root finding, manuscript.

[50]POINCARE, HENRI (1854-1912). French mathematician.

[51]TAGUCHI, G. (1987). System of Experimental Design I & II, UNIPUB Kraus International Publications.

[52] EGGERS, J. AND RIECKE, H. (1999). A continuum description of vibrated sand, Phys. Rev. E. **59** (4), 4476-4483.

[53]GUTMAN, R.G. (1976). Vibrated beds of powders Part I: A theoretical model for the vibrated bed, Trans. Instn. Chem. Engrs. **54**, pp. 251-257.

[54]] MELO, F., UMBANHOWAR, P. AND SWINNEY, H. L.(1995). Phys. Rev. Lett. **75**, 3838.

[55] UMBANHOWAR, P. , MELO, F. AND SWINNEY, H. L. (1996). Nature **382**, 793.

[56] E. CL_EMENT, L. VANEL, J. RAJCHENBACH AND J. DURAN (1996). Phys. Rev. **E53**, 2972.

[57] T. H. METCALF, J. B. KNIGHT AND H. M. JAEGER (1997). Physica. A236, 202.

[58]A.J.LICHTENBERG, M.A.LIEBERMAN.(1992). Regular and Chaotic Dynamics. Springer-Verlag, New York.